Theses of Doctoral (PhD) Dissertation

Hemodynamic and Microcirculatory Effects of a Microsurgical Experimental Carotid-Jugular Fistula

Souleiman Ghanem, MD, MS

Dissertation supervisor: Prof. Norbert Nemeth, MD, PhD, DSc

University of Debrecen
Doctoral School of Clinical Medicine
Debrecen

2021

Table of Contents

The list of abbreviations

AVF	Arteriovenous fistula
ACF	Aortocaval fistula
AVM	Arteriovenous malformation
CCA	Common carotid artery
CJF	Carotid-jugular fistula
CHF	Chronic heart failure
DBP	Diastolic blood pressure
EJV	External jugular vein
EI	Elongation index
EI_{max}	The maximum EI
FG	Fistula group
Hct	Hematocrit
Hgb	Hemoglobin
HIF	Hypoxia-inducible factors
HR	Heart rate
LD	Laser Doppler
MAP	Mean arterial blood pressure
MCH	Mean corpuscular hemoglobin
MCV	Mean corpuscular volume
MPV	Mean platelet volume
Plt	Platelet count
RBC	Red blood cells
RDW	Red Blood Cell Distribution Width
SBP	Systolic blood pressure
SCM	Sternocleidomastoid muscle
SG	Sham-operated group
SPSS	Statistical Package for the Social Sciences
SS	Shear stress
$SS_{1/2}$	Shear stress at half-maximal deformation
WBC	White blood cells

1. Introduction

Arteriovenous fistula (AVF) is a significance modification of the cardiovascular system since it is an early connection between the arterial and venous circulations, thus the blood flows directly from the artery to the vein bypassing the distal circulation.[1–5] The AVF is very common in the clinical practice, since it could be congenital as arteriovenous malformation (AVM) or acquired as hemodialysis fistula, iatrogenic fistula and traumatic fistula.[3–5]

Congenital AVFs are rare and exist usually due to the failure of the differentiation of embryonic vessels into arteries and veins.[3,4] Hemodialysis fistulas provide long-term, high-flow, and easy access for hemodialysis patients without any real alternatives. Therefore, these fistulas are the most common form of AVFs.[5,6] The incidence of iatrogenic AVFs is increasing exponentially due to increased percutaneous interventions and the femoral AVFs are the most frequent form of these fistulas.[3,4] Traumatic AVFs occur in the civilian and military vascular trauma, and can be found in all vessels, especially in the neck and abdomen.[3] Spontaneous AVFs should also be also mentioned, they occurred after the rupture of diseased artery into a contiguous vein.[3,4,7]

Arteriovenous fistula has been and is still the focus of many studies due to the wide spectrum of systemic effects. The systemic effects are not limited to the cardiovascular system, as they involve other neurohormonal and pulmonary effects such as pulmonary hypertension and the changes in natriuretic peptides.[1,8–10] Patients with arteriovenous fistula face in addition to the systemic complications many other local ones as local venous hypertension and mass effects of the fistula.[1]

On the other side, many challenges exist to maintain the patency of the arteriovenous fistula as the only reasonable vascular access in hemodialysis patients. These challenges include recurrent stenosis, thrombosis of the arteriovenous fistula, impaired maturation, access-related complications and intimal hyperplasia.[1]

The fistula-related hypoperfusion or ischemia is one of the important complications. The arteriovenous fistula impairs the distal circulation,[11] and this impairment could lead in 1-9% of cases to critical access-related ischemia.[12,13] It is challenging to manage this kind of ischemia. Although it could actually be managed by the surgical closure or banding of the fistula, but in the case of hemodialysis fistulas, the main challenge is to manage these complications without sacrificing this important hemodialysis access.

Numerous medical studies have been conducted to figure out new aspects that can be used for the management of this hypoperfusion, we intended by this study to approach the fistula-related hypoperfusion from a microcirculatory point of view and to identify the factors affecting the microcirculation. Many animal models were used to study the pathophysiological effects of the AVFs. There is no complete model simulating AVFs in humans, and each model has many disadvantages and advantages. According to our Knowledge, a model to study the microcirculation and rheology has not yet been evaluated. A carotid-jugular fistula (CJF) model will be tested in this study as a feasible model for such studies.

2. Literature review

2.1. The impact of arteriovenous fistulas on distal microcirculation

A combination of systemic and local factors plays an important role in fistula-related hypoperfusion, however the full pathophysiology is not fully clear, and it is unknown why these ischemic symptoms occur in some patients and do not occur in others.[12,14]

The systemic cardiovascular changes are undoubtedly an important cause of this ischemia, especially mean pressure drop in the case of AVF. There are also several other mechanisms by which the fistula affects the microcirculation distal to the fistula, such as the tendency of blood to flow into a low-resistance vein rather than a high-resistance artery, or the so-called steal syndrome. Other vascular mechanisms may also contribute such as the presence of concomitant atherosclerosis.[15] Other mechanisms are known in patients with chronic kidney disease, such as the high level of urea, and some studies have shown the negative effect of the chronic kidney disease on microcirculation.[16] The change of local vascular resistance and tone due to the imbalance between vasodilators and vasoconstrictors also leads to important changes in the microcirculation.[10]

The proposed mechanism in our study is that the impairment of the rheological properties of erythrocytes due to high shear stress could worsen the microcirculation (see Figure 1).

The microcirculation is a peripheral vascular network with diameters less than 100 μm.[17] Malpighi in 1660 was the first to see the microcirculation and microscopically proved the existence of a connection between the arterial and venous sides of the circulation through a network of microcirculations.[18] Since that time, the microcirculation and its vital role in the functions of individual organs and the life of the whole organism have become clearer. Many biological mechanisms take place in the microcirculation, such as gas and nutrients exchange, regulation of vascular tone, transport of all blood-borne hormones and mediating the functional

activity of the immune system and hemostasis.[17,19] Many new treatments are also based on improving the microcirculation, and the microvascular dysfunction is considered as one of the important pathophysiological mechanisms for many diseases and a risk factor for many disease.[17,19–21]

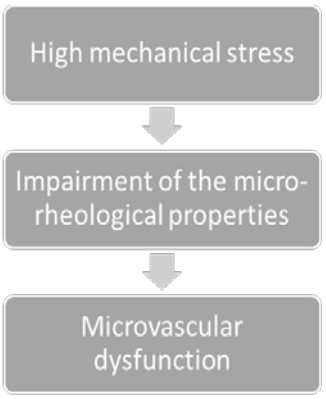

Figure 1. A proposed mechanism for microvascular dysfunction in the presence of an arteriovenous fistula

2.2. Potential effects of arteriovenous fistulas on microcirculation at the rheological level

As we mentioned, the main idea of our study was to evaluate another mechanism of fistula-related hypoperfusion at the microcirculatory level. This idea has come through several studies conducted in our department about the effect of systemic diseases in general and vascular diseases in particular on the rheological properties of erythrocytes and the further consequences of these changes on the microcirculation. A brief review of the theoretical basis of this idea is presented below, by talking about the proposed effects of AVFs on the erythrocytes and subsequently the impacts of the erythrocytes properties on the microcirculation.

2.2.1. The effect of arteriovenous fistulas on erythrocytes properties

AVF affects markedly red blood cell (RBC). Some of these effects are mechanical effects, others are mediated by molecular mechanisms.[22] Blood flows through the AVF at high velocities due to the large pressure gradient between the artery and the vein, this high-velocity flow leads to high shear stress and turbulent flow. Other mechanical effects in human include

the effect of the extracorporeal circulation and the peripheral dialysis needles.[23] All these stresses could cause intravascular hemolysis, and if they weren't high enough to disrupt the RBC membrane, they could result in alteration in the rheological properties and the metabolism of RBCs.[24] The fistula has also effects on RBCs through other pathways such as inflammation and hypoxia.[1,22]

According to our knowledge, several studies focus on the effects of RBC properties on the AVF,[25,26] or on the effects of AVF on gene expression,[27,28] but there is a lack of studies about the effects of AVF on erythrocytes properties.[29]

2.2.2. The effects of erythrocytes properties on blood circulation

Blood circulation could be imagined as an electrical or fluid circuit consisting of three main components: heart as a pump, the conducting vessels as pipes and the blood as a fluid. None of the three components of this circuit can operate independently without affecting or being affected by the other two factors.[30] The rheology is the branch of science concerned with the study of the flow of the fluid. In hemorheology the fluid is blood, and it is classically summarized by studying the blood viscosity.[30,31] The micro-rheologic properties of RBCs are the properties that influence the microcirculation.[11,32–34]

Blood viscosity is the resistance of blood to flow, represents the thickness and stickiness of blood and is directly related to the microcirculation, as shown in Figure 2.[35,36] On the other hand, blood viscosity is a dynamic property of blood, not like osmolality, glucose, creatinine and plasma proteins are static properties,[35] and many factors influence its value, some related to the erythrocytes such as erythrocyte aggregation and deformability and hematocrit, and some not related as plasma viscosity and shear rates.

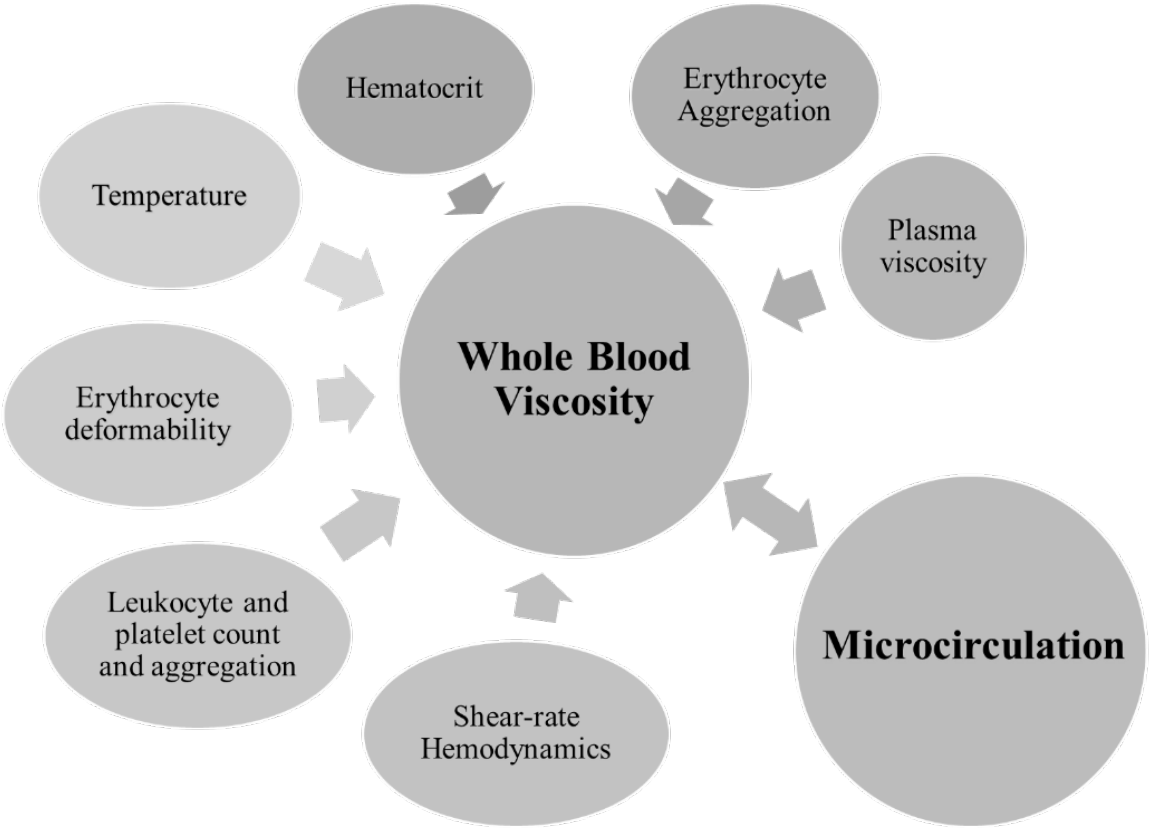

Figure 2. A summary of the most important factors affecting whole blood viscosity and the interactions with microcirculation (Based on Bogár, 1999).[37]

There are many reasons making red blood cells the most important component in determining blood viscosity: First, the big fraction volume in comparison with other blood components such as WBCs and platelets which form about 1% of the total blood volume. Secondly, the unusual shape of RBCs as biconcave discs so they could align with the direction of flow. Thirdly, their ability to change their shapes and to adhere together. Fourthly, their content of high concentrations of hemoglobin which influence on the speed of shape changing under shear forces.[30]

Therefore, the role of RBCs is not limited to transferring the oxygen, but RBCs have also effects both on microcirculation level due to their deformability and aggregability and on large vessels' level mainly by the mass of RBCs.[25,30,38] The ability of RBC to change its shape is very important to enter micro vessels with diameter equal or less to the diameter of RBCs,

while the mechanism of the effect of the RBCs aggregation on the microcirculation is not well understood yet.[39] Impaired rheological properties also contribute in thrombosis formation.[26,40]

RBC mass also affects markedly the blood viscosity thus blood flow. Therefore, one of the open question is the appropriate hematocrit level for fistula patient, since low hematocrit prevents microcirculatory stasis but reduces tissue oxygenation, while high hematocrit enhances oxygen transport but lead to an increased blood viscosity with a concomitant increase in tissue hypoxia.[24,41–44]

This relationship between hemorheological alterations and blood flow is not unilateral but could be considered as a "vicious circle", as shown in Figure 3. The impaired rheological properties affect the blood flow, and the low blood flow leads to local hypoxia, local acidosis, accumulation of metabolic wastes, acute phase reaction and/or leukocyte activation, which in turn impairs the rheological properties.[24]

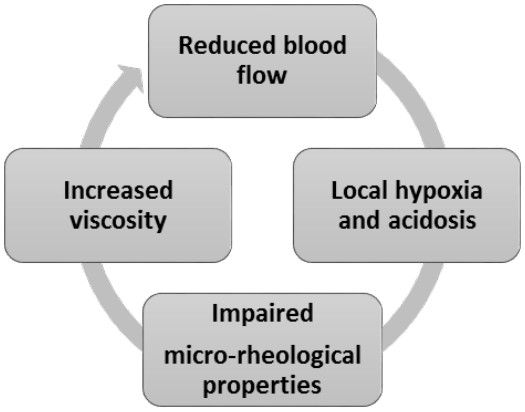

Figure 3. Hemorheological Vicious Cycle[24]

2.3. Methods for evaluating distal microcirculation

The microcirculation of the patients with chronic kidney disease and hemodialysis was evaluated in several studies using different methods such as *in-vivo* microscopy, side-stream dark field imaging Laser, Laser Doppler fluximetry and Laser Doppler Line Scanner.[15,16,45,46]

2.3.1. Laser Doppler

The laser Doppler is a good instrument for evaluating the microcirculation and for studying fistula-related hypoperfusion. It was developed in the late 1970s and uses the same principle as Doppler ultrasound, it measures the frequency shift of light when it is reflected back from moving particles such as red blood cells, so we can calculate the velocity and concentration of these globules.[47,48]

The values of the waves were expressed in Blood Flux Units (BFU [au]), which is determined by the velocity and number of the moving red blood cells (RBCs) in the examined tissue. There are some technical matters that must be taken into account when using laser Doppler, such as the distance of the probe from the tissue, the pressure of the probe on the tissue, artificial motion, and the calibration of the instrument.[49,50] Many of the surrounding conditions must be adjusted during the measurement process to obtain accurate measurements, such as room temperature, moisture at the measurement points and performing the measurements always at the same anatomical site.[51]

The microcirculation in studies was evaluated in different locations such as the microcirculation proximal and distal to the fistula and sublingual microcirculation. These studies have generally shown heterogenous results but tend to show a decrease in both the general microcirculation and the microcirculation distal to the fistula in patients with chronic kidney disease and/or AVFs.[45,46,52]

2.3.2. The consequences of the acute arteriovenous occlusion

We assumed that more information about the microcirculatory status will be available from studying the microcirculatory changes after the acute occlusion of the arterial limb of the fistula since the occurrence of such acute changes will provide clear evidence of the significant role of these fistula on the microcirculation.[53]

The acute occlusion of the AVF provokes significant hemodynamic changes immediately after one or two heart beats. These changes include change both the heart rate and the blood pressure. Many Studies were conducted to explain these changes.[53] However, The physiological mechanism of these changes remains unclear.[54] The acute occlusion releases complex processes mainly the sudden increase of the afterload, other processes should be mentioned such as stimulating the baroreceptors mediated through the vagal nerve, releasing chemical substances (acetylcholine, 5-hydroxytryptamine) and sudden decreases in NO production.[53]

2.4. Other important aspects about arteriovenous fistulas

We aimed in this study also to prove the significant effects of our model on both the microcirculation and the structure of the remote organs thus to present this model as a feasible model for such studies.

2.4.1. The structural vascular changes

The AVFs lead to a complex remodeling of the vascular system, where the initial changes include a redirection of the blood flow towards the low resistance circulation in the vein. These changes are followed by structural and functional changes of the vein and artery, or the so-called maturation of the fistula, including increasing the diameter of the artery and vein as well increasing the blood flow though the fistula. The blood flow increases usually by 10 to 20 times to reach 500-200 milliliters per minute in Cimino fistula, and 500-3000 ml per minute in upper arm fistula.[10,11,15]

2.4.2. The systemic effects of arteriovenous fistula

Arteriovenous fistula (AVF) is known of its immediate and late systemic effects which contribute to morbidity and mortality especially in the presence of high-flow fistula, prosthetic grafts or other comorbidities.[1,3,55] These effects are mediated by significant pathophysiology

changes in the cardiovascular system altering systemic hemodynamic status, altering the cardiac load by increasing the preload and decreasing the afterload and altering the level of some vasodilators and vasoconstrictors such as nitric oxide.[8,9] Some studies showed that AVF could reduce also the coronary perfusion especially in the subendocardial region.[8]

The effects of AVF involve also pulmonary effects such as pulmonary hypertension and the changes in natriuretic peptides. The pulmonary hypertension could be related to the fluid overload, hemodynamic changes, decreased nitric oxide production and endothelial dysfunction.[1]

The arteriovenous fistula has other effects by bypassing the distal vascular beds inducing fistula-related hypoperfusion.[12,13] Steal syndrome is the main mechanism to explain this hypoperfusion and may lead to ischemic changes and impairment in the microcirculation.[11,12]

2.5. Arteriovenous models

2.5.1. General models

Many models have been developed for AVFs studies. Although these models in large animals are technically easier and closer to the human AVF, but they cost more and require higher technical expertise and equipment. In addition, it is difficult to establish a mixed diseases models in large animals. All these reasons limited the use of these models and increased the popularity of models of AVF in small animals.[9,56,57]

A lot of models are described in rats such as the aortocaval model (ACF), the tail model and models in the carotid or femoral regions. The advantages and disadvantages of each model should be taken into consideration by designing the study. Although the recent technique to construct ACF is more simpler and faster,[56,58] this AVF represents a fistula in centrally located vessels as opposed to AVF in humans.[59] Furthermore, it requires a laparotomy,[56] and the

construction of ACF by puncturing technique could cause higher rate of failure not related to the fistula dysfunction itself but to the higher technical failure.[58]

Regarding to the tail-vein model in addition to the technically challenging,[58,60] Beatty et al. described some technical problems limit the usefulness of this model, including thrombosis, desiccation and the development of dense scar tissue that could compress the vessel.[60]

Femoral AVF is one of the most used model, but it may lead to arterial ischemia or to venous hypertension.[9,61] The anastomosis can also be more challenging due to the thin and collapsible wall of the femoral vein in comparison with human veins or with external jugular vein (EJV) in rats.[62]

2.5.2. Why carotid-jugular fistula?

We chose this type of fistula for many reasons. First, the unilateral carotid ligation in rats is almost innocuous.[63] Second, the neck is a clean area with good perfusion, which permits a rapid and uncomplicated wound healing, in addition to the avoidance of unnecessary laparotomy. Third, the external jugular vein could be easily isolated because it is not accompanied by artery or nerve, and its thick wall and large diameter make the anastomosis easier and its structure resembles the superficial veins in human.[62] Fourth, although the CJF is considered as a large AVF as ACF, its anatomical location is closer to Cimino fistula in human since both of them located on the aortic arch branches.

2.5.3. Literature review of carotid-jugular fistula

The carotid-jugular fistula is a known model in the literature decades ago, and the applications of this model differ according to the method of conducting the anastomosis. The oldest and most common application is as a model for arteriovenous malformation,[64] and there

are other applications, for examples to study cerebral venous hypertension, chronic cerebral hypoperfusion, arterial dilatation and AVF.[65–68]

A search for related articles was performed in PubMed up to 12th July 2017 and the following search term was used (carotid AND jugular AND Rat AND fistula). The search result was 39 items, but one is excluded because it is about intestinal transplantation. The table (1) summarizes these studies. A further study was added to this table about the application of this fistula as a model of chronic heart failure.

There are many studies which have used carotid jugular fistula as a model, but the applications of this model differ according to the direction of the blood flow. The applications of this model could be divided into two groups a) model of arteriovenous malformation or cerebral venous hypertension where the direction of blood is towards the distal end of the jugular vein i.e. towards the brain veins. This model was the most common used application of this fistula b) model of AVF or heart failure where the direction of blood is towards the proximal segment of the jugular vein i.e. towards the right atrium. The carotid jugular fistula in the current study was added to the table as a model of AVF.

Table 1. Summary of some studies about carotid jugular fistula.

Model	direction of blood flow to	Anastomosis			Articles (Model) (artery to vein) (technique)
		CCA to EJV	Side	Technique	
AVM CVH CCH	The brain / Distal end of EJV	End to End	Right	Ascending aorta graft - Suturing	(AVM) (P to D) (ascending aorta graft): Lawton MT.[69,70] (AVM) (P to D) (suturing): Shin Y,[71,72] Zhu Y,[73] Yamada M,[74] Herman JM,[75] Bederson JB.[76] (CCH) (D to D): Sekhon LH,[66] Irikura K,[77] Morgan MK. [64,78–80]
		Side to End	Left or Right	Suturing	(AVM) (S to D) (Left): Raoufi Rad N,[81] Yassari R,[82] Kashba SR,[83] Terada T,[84] Ng K,[85] Tu J,[86,87] Karunanyaka A,[88] Storer K.[89] (AVM) (S to D) (Right) Hai J.[90–93]
		End to side	Right	Suturing	(CVH) (P to S + ligating P of EJV): Yang ST.[94]
		Side to side	Left	suturing	(CVH) (S to S + ligating P of EJV) Kojima T,[95] Sahara Y.[67]
AVF AD CHF	The heart / Proximal end of EJV	End to end	Right	Cuff technique - Suturing	(AVF) (P to P) (cuff technique): Zheng Cs.[57] (AVF) (P to P) (suturing): current study.
		Side to End	N	Suturing	(AVF) (S to P + ligating D of CCA): Geenen IL.[96]
		End to side	Right	Suturing / introducing	(AVF) (P to S + ligating D of EJV) (suturing): Chien CT.[97] (CHF) (P to S) (Introducing the artery into the vein): Chou TF.[98]
		Side to side	Left	Suturing	(AD) Tohda K,[68] Sageshima M.[65]

AVM, arteriovenous malformation, CVH, cerebral venous hypertension, CCH, Chronic Cerebral Hypoperfusion, AVF, arteriovenous fistula, AD, arterial dilatation, CHF, chronic heart failure, CCA, Common carotid artery, EJV, External jugular vein, N, not identified, P, proximal end, D, Distal End, S, side. Note: Proximal: The end situated nearer to the center of the body or caudally (there is widespread confusion about the meaning.[99])

Objectives

1. The main aim of this study was to evaluate another mechanism of fistula-related ischemia at the microcirculatory level. Our hypothesis was that the high turbulent flow through the arteriovenous fistula worsens the micro-rheologic properties of RBCs as a suggested mechanism of impaired tissue perfusion.
2. This study was also conducted to check the feasibility of carotid-jugular fistula (CJF) as a model to study fistula-related microcirculatory and systemic changes, thus a feasible model to test our hypothesis.
3. Another purpose was to show the effect of arteriovenous fistula on the hemodynamic and morphology of remote organ as well as to compare our results with other fistula models in rats.

3. Materials and methods

3.1. Experimental animals

The experiments were done at the Department of Operative Techniques and Surgical Research and registered by Committee of Animal Welfare at the University of Debrecen, (Registration Nr.:25/2016/DEMÀB) according to the Hungarian Animal Protection Act Law XXVIII/1998, EU Directive 2010/63/EU and the Ordinance 40/2013.

Wistar (Crl:WI) rats were used in this study, the rats were healthy female at 10-12 weeks of age. The total number of experimental animals was sixteen, ten rats in the fistula group with an average weight of 272±22 g (FG, n=10) and six rats in the sham-operated group with an average weight of 267±11 g (SG, n=6). The rats were acclimated for two weeks with natural day/night cycle. Standard cages were used for housing with free access to water and commercially food.

The anesthesia protocol included the administration of sodium thiopental (60 mg/kg, intraperitoneal, Thiobarbital 0.5 g, B. Braun Medical S.A., Spain) and Atropine (0.05 mg/kg subcutaneous). The goal of Atropine is to prevent bradycardia and airway secretion. All stages of follow-up were done by the same anesthesia protocol.

3.2. Operative techniques

The surgery was done in sterile conditions and gauzes were used as operation towels. The right side of the neck and upper chest was shaved and disinfected with Betadine®. An oblique surgical incision, about 1.5 cm in length, was made at the lower part of the neck just above the right clavicula and the sternal notch. The subcutaneous tissue was cut in the medial part of the incision up to the level of sternocleidomastoid muscle (SCM), the remaining lateral part of the subcutaneous tissue was then lifted using anatomical forceps and cut at the same level. The right EJV appears usually in this plane lateral to SCM. The vessels should be gently

isolated with a lot of attention, the vein was isolated carefully to its large tributaries i.e. for about 7 mm above the clavicle. After enough preparation of the vein, the right common carotid artery (CCA) was isolated medial to the SCM for about 10-12 mm above the clavicle. The distal ends of both artery and vein should be ligated, since we intend to make anastomosis between the proximal ends of the artery and vein. The CCA ligation was located as distal as possible, and the EJV was ligated just under the tributaries. The proximal parts of both the artery and vein should be controlled using fine clamps. Two temporary clips were used for the artery and one clip for the vein. The artery was cut a 45-degree angle medially and obliquely (see Figure 4) so that the artery diameter matched to the diameter of the vein. The EJV was cut perpendicular under the ligation. Any traces of blood in the lumens of both artery and vein were removed and irrigated with sodium-heparin solution (10 U/ml). An end-to-end anastomosis was constructed in front of SCM between the proximal ends of artery and vein with continuous suture using 10-0 polyamide suture material (Silon, Chirmax, Prague, Czech Republic). The clips were released after the construction of the anastomosis to check any bleeding from the anastomosis. The fistula should be observed for few minutes to check the patency or any further bleeding. The skin was closed with continuous suture using a 4-0 Glycolide-ε-Caprolactone (Monolac, Chirmax, Prague, Czech Republic). Figure 4 shows the construction of the fistula step by step using operating microscope. Figure 5 shows demonstrative representation of CJF.

The blood loss was replenished using normal saline solution subcutaneously to, and Flunixin (2.5 mg/kg, s.c.) was administered after the surgery for pain management. The rats were returned after recovery to individual cages. They were then subjected to regular monitoring as well as wound care.

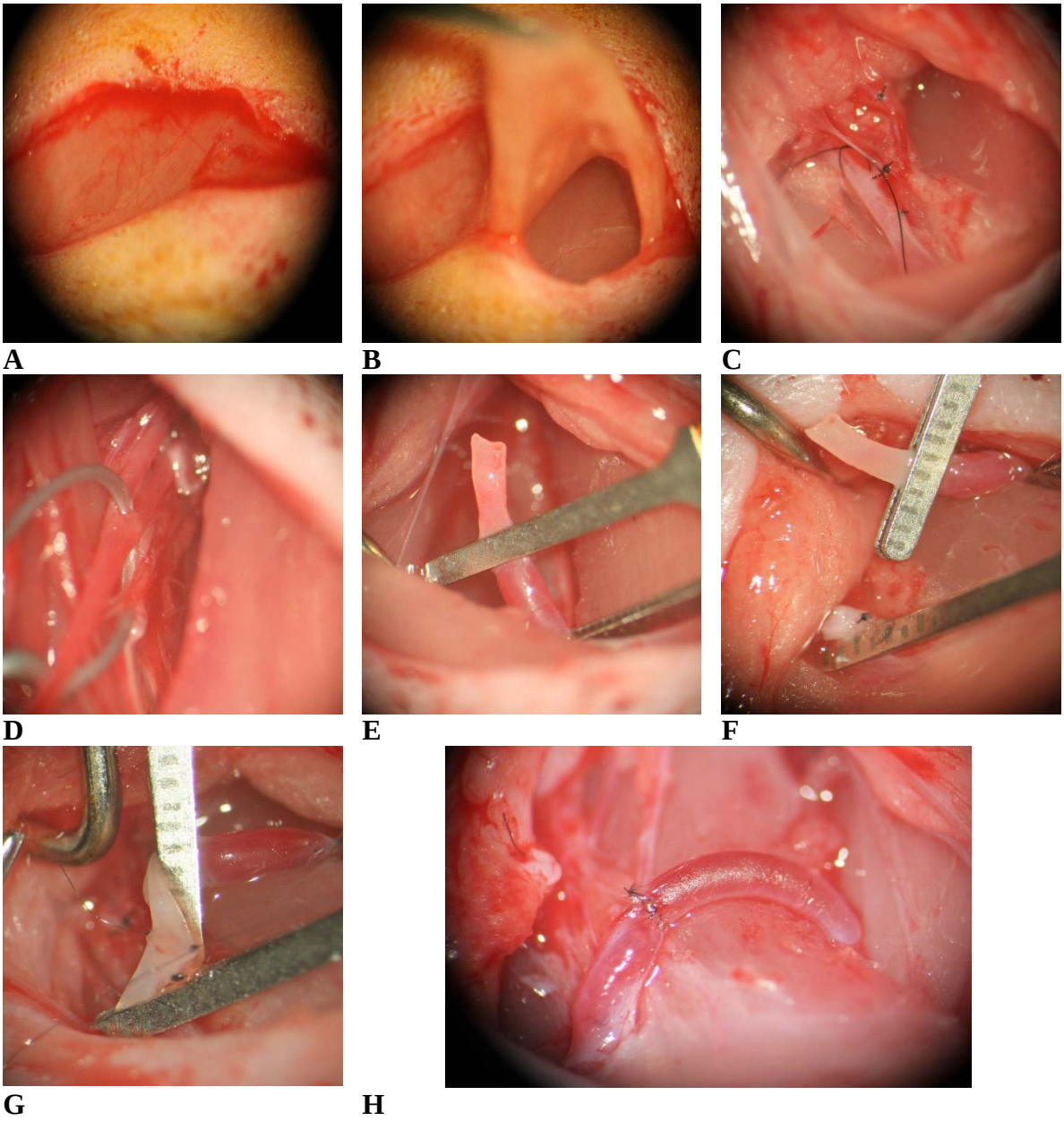

Figure 4. Photos for the operative steps taken under microscope from A to H as following: (A) a single supraclavicular incision (B) First cut the subcutaneous medial (C) Isolated and prepared external jugular vein (D) Isolated and prepared common carotid artery and its bifurcation (E) Cut the end of the artery at an angle of 45-degree (F) Approximation of the artery and vein (G) Two holding stitches (H) Carotid-jugular fistula

The rats in the SG were subjected to the same surgical protocol in terms of preparation, surgical incision and vessels isolation, but without any further other vascular interventions such as ligation, clamping, or anastomosis.

This experiment was done under an operating microscope (Leica Wild M650, LEICA Ltd., Germany), with documentation be photos and video. The diameter of CCA and EJV was measured by a scaled clip, the diameters were in average 1 and 1.5 mm respectively.

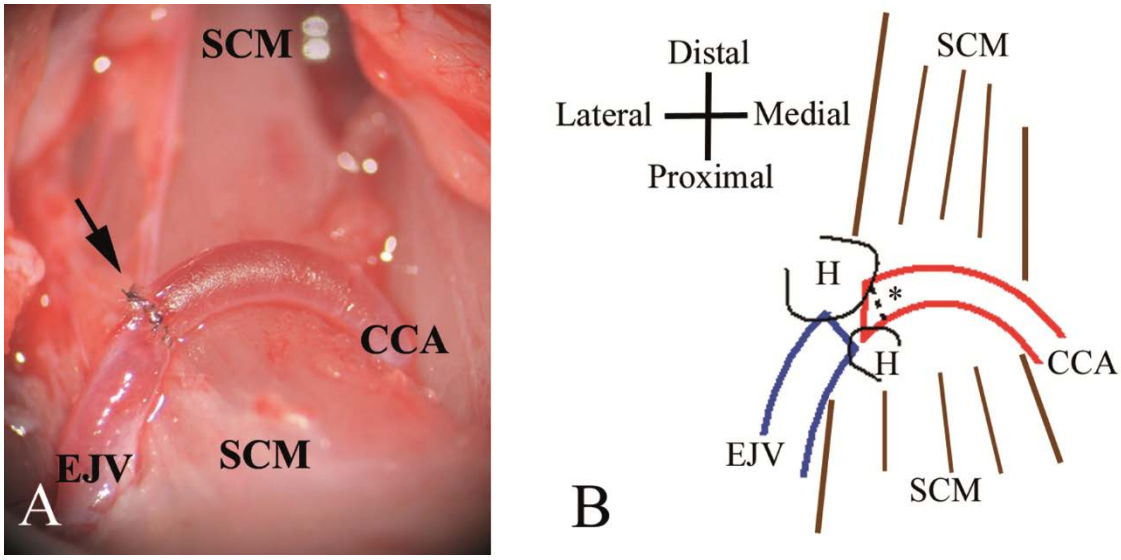

Figure 5. (A): Intraoperative photo of carotid-jugular fistula directly after the construction of the fistula. (B): Schematic representation of the previous photo. Black arrow: the anastomosis. SCM, sternocleidomastoid muscle. CCA, common carotid artery. EJV, external jugular vein. H, holding stitch. *, Cut the end of the artery at an angle of 45-degree (dashed line shows the perpendicular level).

3.3. Follow-up protocol

The follow-up period was 6 weeks and was determined after reviewing the literature to achieve the goal of the study by evaluating the isolated effects of arteriovenous fistula, in other words before the developing of heart failure, approximately 8 weeks.[100] The measurements were carried out before the construction of the fistula as baseline measurement (FG-base and SG-base) and one week after the surgery (FG-1W and SG-1W) and six weeks after the surgery (FG-6W and SG-6W).

The measurements included the following: neurobehavioral assessment, evaluation of the patency of the fistula, evaluation of the microcirculation by laser Doppler, hemodynamic measurements, weight measurements, hematological and hemorheological measurements. The

rats were sacrificed by exsanguination at the end of the measurements, i.e. at the 6th week follow-up, then we have taken tissue samples for histologic studies.

3.4. Neurobehavioral assessment

Garcia scale was used for the neurological examination of these rats, which has been used in many studies on neurological diseases in rats.[101–104]

Table 2. The neurobehavioral study for right transient ischemic attack.[102]

Test	Score			
	0	1	2	3
Spontaneous activity (in cage for 5 min)	No movement	Barely moves	Moves but does not approach at least three sides of cage	Moves and approaches at least three sides of cage
Symmetry of movements (four limbs)	Left side: no movement	Left side: slight movement	Left side: moves slowly	Both sides: move symmetrically
Symmetry of forelimbs (outstretching while held by tail)	Left side: no movement, no outreaching	Left side: slight movement to outreach	Left side: moves and outreaches less than right side	Symmetrical outreach
Climbing wall of wire cage	…	Fails to climb	Left side is weak	Normal climbing
Reaction to touch on either side of trunk	…	No response on left side	Weak response on left side	Symmetrical response
Response to vibrissae touch	…	No response on left side	Weak response on left side	Symmetrical response

This scale includes six components: spontaneous activity, symmetry in the movement of limbs, forepaw extension, climbing, body proprioception and response to vibrissae touch. The maximum score for each component is 3 and the minimum score is zero or one, and the minimum overall score is 3 and the maximum is 18.[101,102]

3.5. Evaluation the patency of the fistula

After the operation, the fistula was checked by milking test (clamping the vein after the anastomosis with first forceps then emptying the vein of blood by squeezing the vein with second forceps for a few millimeters from the first forceps. The fistula is patent when the vein refills quickly after the releasing of the first forceps). This test is also called empty and refill test.

The patency of AVFs was confirmed at the first week follow-up by the physical examination and handheld Doppler. At the sixth week follow-up, the fistula was isolated through a small incision to check the patency by the pulsatile appearance and milking test.

3.6. Laser Doppler measurements

This microcirculation was evaluated by the laser Doppler, and this evaluation was carried out by the recording of laser Doppler waves from the organs distal to the fistula, in other words the microcirculation of the liver and kidney. We have chosen these organs since they are the first suitable and measurable organs distal to the origin of the fistula. In addition to the availability of the required expertise and tools for these measurements at our department.

The microcirculation was evaluated only at the end of the experiment in both groups, since it needs an invasive procedure, a laparotomy. The fistula was approached at the beginning through an incision about 1 cm above the right clavicle, and total isolated from the surrounding tissues. After that, the abdominal cavity was opened through midline incision, and the microcirculation was measured using the laser Doppler on the anterior surfaces of the right kidney and liver at the 6^{th} week follow-up. These measurements were once again repeated after the occlusion of the arterial limb of the fistula and the CCA using temporary clip in FG and SG, respectively. The laser Doppler (LD) tissue flowmetry (LD-01, Experimetria Ltd., Hungary) was used (see Figure 6) with a standard pencil probe (Oxford Optronix Ltd., UK).

S.P.E.L. Advanced Kymograph software (Experimetria Ltd., Hungary) was used to record the measurements and analyze the values of the waves.

A

B

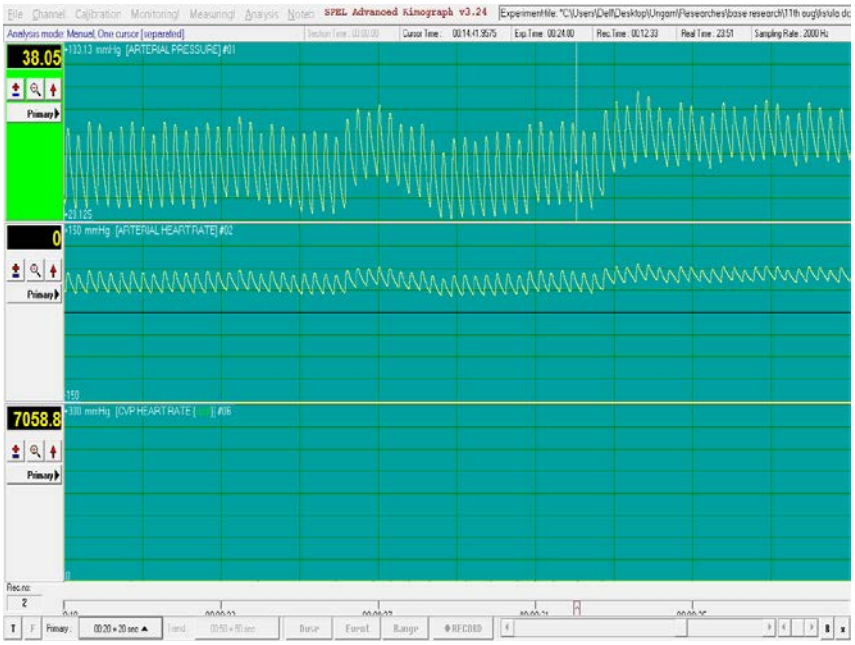

Figure 6. A: The laser Doppler tissue flowmetry. **B:** S.P.E.L. Advanced Kymograph software.

After the stability of the laser Doppler waves, a period of 10-second was recorded, and the mean values of this period was used as laser Doppler value for each measurement. The values of the waves were expressed in Blood Flux Units (BFU [au]).

3.7. Hemodynamic measurements

Hemodynamic measurements in our study included measurement of systolic and diastolic pressure and heart rate. Two systems were used in these measurements, non-invasive and invasive system. The non-invasive system was used for the baseline measurement and 1st week follow-up, the measured parameters were systolic blood pressure (SBP) and heart rate (HR). These measurements should be done under ambient temperature of 30 °C. The method of measurement was a non-invasive tail cuff method by using a non-invasive Blood Pressure Amplifier (Apollo, IITC Inc., CA, USA). This device involves an artifact filter, which minimizes the artificial movements.

The invasive System was used at the 6th week follow-up by placing the catheter in the abdominal aorta. The used device was (LD-01, Experimetria Ltd., Hungary), and G20 cannula was used as catheter. The following parameters were measured through the invasive system: systolic (SBP) and diastolic blood pressure (DBP) and HR, the same measurements were repeated once again after the acute occlusion of the arterial limb of the fistula in FG or the CCA in the SG. The results for 10 seconds were analyzed for each case in the invasive measurements, the average of the maximum pressure values was considered as SBP value, the average of the minimum pressure values for the same period was considered as DBP value, and the average of seven measured HR values was considered as HR value.

A

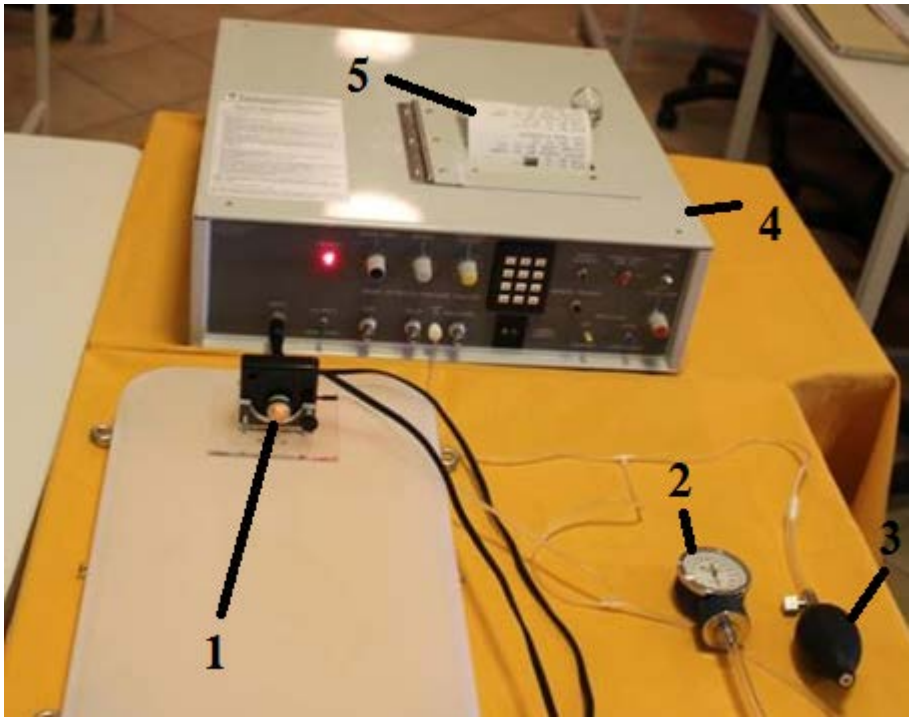

B

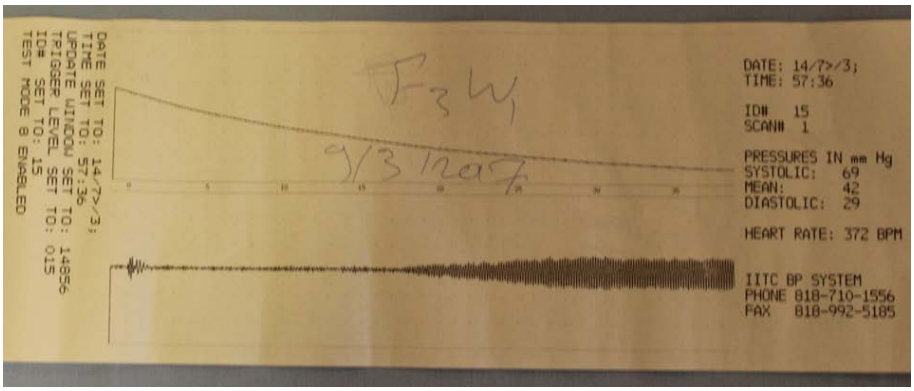

Figure 7. A: The non-invasive system for hemodynamics measurements. 1: the cuff. 2: the manometer. 3: Inflation bulb. 4: the machine. **B:** the printed results show the detected pulse waves.

3.8. Blood sampling

The blood samples were venous at all stages and were taken without using of tourniquets. Blood samples for the baseline measurements were drawn from the lateral tail veins or directly from the isolated vein during the surgery. The blood samples were drawn on the 1st week postoperative week from the lateral tail veins (about 0.3 ml, as non-terminal sampling), and on the 6th week postoperative from caudal vena cava (about 2-3 ml, as terminal sampling). BD Vacutainer® tubes were used (K3-EDTA 5.4 mg / 3 ml). The laboratory measurements were begun within 30 minutes after blood sampling.

3.9. Hematological measurements

Hematological parameters were tested using (Sysmex F-800 automate, Sysmex Co., Ltd. Japan, see Figure 8). The measurement requires about 70 µl of blood. The studied parameters were: white blood cell count (WBC [10^3 / µl]), red blood cell count (RBC [10^6 / µl]), hemoglobin (Hgb [g / dl]), hematocrit (Hct [%]), mean corpuscular hemoglobin (MCH [pg]), mean corpuscular volume (MCV [fl, Femtoliter]), mean corpuscular hemoglobin concentration (MCHC [g / dl]), red blood cell size distribution (RDW-CV%), platelet count (Plt [10^3 / µl]) and mean platelet volume (MPV [fl]).

Figure 8. The used device to measure the hematological parameters
(Sysmex F-800 automate, Sysmex Co., Ltd. Japan)

3.10. Hemorheological measurements

The RBC deformability was evaluated using laser diffraction ektacytometry technique. This technique allows us to measure the elongation of the RBCs shape at a specific shear stress using a laser diffraction pattern.[105]

LoRRca MaxSis Osmoscan (Lorrca®) is used in our department, manufactured by Mechatronics BV in the Netherlands (Lorrca is the acronym for Laser Optical Rotational Red Cell Analyzer). The test requires a highly diluted blood sample, 10 µl of blood mixed in 2 ml of polyvinylpyrrolidone (PVP) - phosphate buffered saline (PBS) (viscosity: 27 mPas,

osmolarity: 300 mOsm / kg, pH: ~ 7.3). The RBCs are exposed to increased shear stress (SS), the elongation of the RBCs is measured at different shear stresses in the range from 0.3 to 30 Pa. The data are presented as EI-SS curves.[47]

Each case is represented by a curve, and the cases would be compared by comparing these curves. We compare these curves with some parameters, the maximum elongation index (EI_{max}), the shear stress corresponding the half of the maximum elongation index ($SS_{1/2}$ [Pa]) and the ratio between EImax and SS1/2. These parameters are calculated using Lineweaver-Burke analysis: $1/EI = (SS_{1/2}/ EI_{max}) \times (1/SS) + (1/EI_{max})$.[106,107]

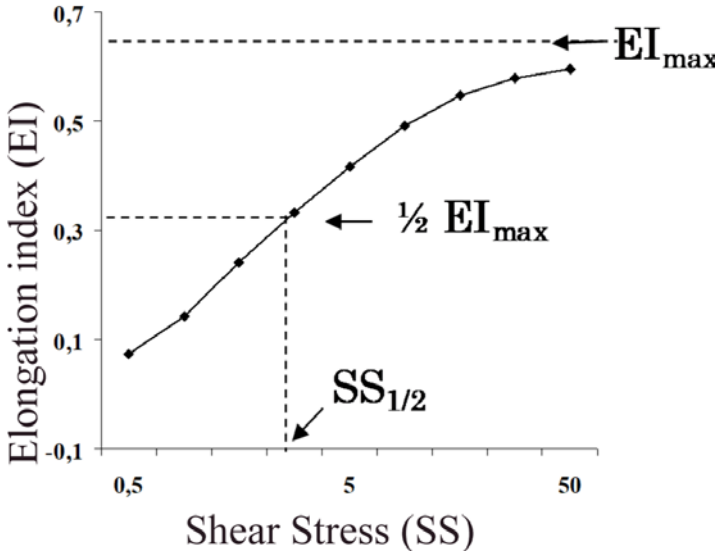

Figure 9. Typical curve of Elongation index - Shear stress [Pa] (Based on Baskurt 2009).[106]

The mechanical stability of the membrane was evaluated by subjecting the RBCs to a high mechanical pressure (100 Pa, 300 s) and comparing the deformation of the RBCs before and after.[108] The above-mentioned parameters (EI values, EI_{max} and $SS_{1/2}$) were compared and the ratio between before and after was calculated.

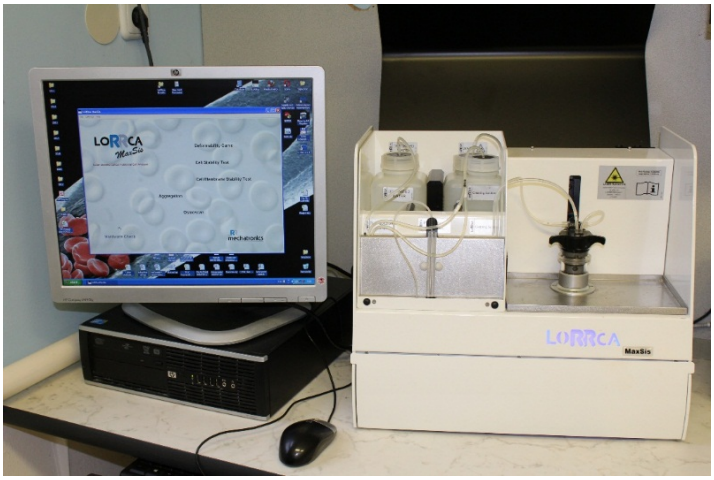

Figure 10. Laser-Assisted Optical Rotational Cell Analyzer (LORCA) to measure the RBC deformability and membrane stability

3.11. Density separation of RBC subpopulations

We assumed that more information will be available from studying the hemorheological differences between RBCs subpopulations, since the AVF could influence on the old RBCs populations through some mechanisms such as intravascular hemolysis.

The measurements of density separated RBCs require 2-3 ml of blood. This amount of blood is quite large relatively to rats, so these measurements were performed on other six healthy female rats as a negative control group (CG, *n*=6, bodyweight: 271.33±11 g) and on 5 rats of FG-6W. About 2-3 ml of blood was drawn from the caudal vena cava, and hematological and hemorheological measurements were done. The rest of the sample was centrifuged at 4000 rpm (1800 g) for 60 min using centrifuge (Hettich Universal 32R, Germany), the layer of clear fluid (plasma) was aspirated and kept aside, and the 'buffy-coat' was removed. Since rat blood cells are known to be sensitive for physical effects, we did not wish to use centrifugation at higher force.

Ten percent of RBCs was calculated depending on the base values of Hct and sample size. This percent was aspirated from about the top 10% and bottom 10% of the RBC column. Top RBCs were considered as dominantly 'young' RBCs and bottom RBCs were considered

as dominantly ‘old’ RBCs.[47] Top and bottom samples were diluted in autologous plasma adjusting the Hct to 40%.

3.12. Hematocrit standardization

The effect of hematocrit on rheological parameters has been the focus of several studies. Here we intended to conduct a more in-depth study of the results of the previous step to find out the effect of hematocrit on the RBCs deformability.

The samples of the young and old RBCs were considered a representative of standardized Hct in both groups, where the hematocrit value is 40%, and the RBCs deformability was measured in these samples. The RBCs deformability was measured in the native samples before hematocrit standardization as well. The RBCs deformability was then compared between before and after Hematocrit standardization.

3.13. Weight measurements

Body weight was measured at each stage of the study (Base line, 1st and 6th week postoperative). The weights of the organs (heart, lungs and liver) were measured only at the 6th week follow-up at the end of the experiments. The relative weight of the organs was calculated by dividing the absolute weight of organs by the body weight and used to compare the groups. Organs weight was measured by using Analytic scale (LMIM, LB-1050, Hungary).

3.14. Histological examinations

Tissue samples were taken at the end of the experiment and fixed in 4% buffered formaldehyde solution. These samples included the excision of the hearts and the vessels mentioned later. Histology slides were scanned using the following device (Pannoramic MIDI II, 3DHISTECH Ltd, Hungary) and this software (Pannoramic Viewer, 3DHISTECH Ltd, Hungary) was used to for the measurements.

The sections of the Hearts were stained using Hematoxylin and Eosin (H&E). The thickness of the left ventricular wall was measured in 4 different points and the thickness of the right ventricular wall was measured in 3 different points.

Vessels samples were also taken to compare the intima thickness of the venous limb of the fistula with the contralateral vein (non-operated EJV in FG) and with the vein in SG (right EJV). Elastic Van Gieson (EVG) was used to stain these sections. The thickness of the intima was measured in ten points and the mean of highest three measurements for each sample was considered as intima thickness.

3.15. Documentation sheet

All the data obtained from the experiments was documented in one application, such as vital parameters, operation notes, neurological assessments and the medications, see Figure 11. All stages of the experiment were documented in the same form.

3.16. Statistical analysis

The results were expressed as means ± standard deviation (SD). For normally distributed data, the paired samples T test was used to compare two paired samples and the one-way ANOVA test was used to compare two independent samples. For non-normally distributed data, the Wilcoxon signed-rank test was used to compare two paired samples and the Mann-Whitney U test was used to compare two independent samples. $P<0.05$ was considered statistically significant. IBM SPSS Statistics version 22 was used for the statistical analysis and Microsoft Excel 2016 was used for designing the graphs.

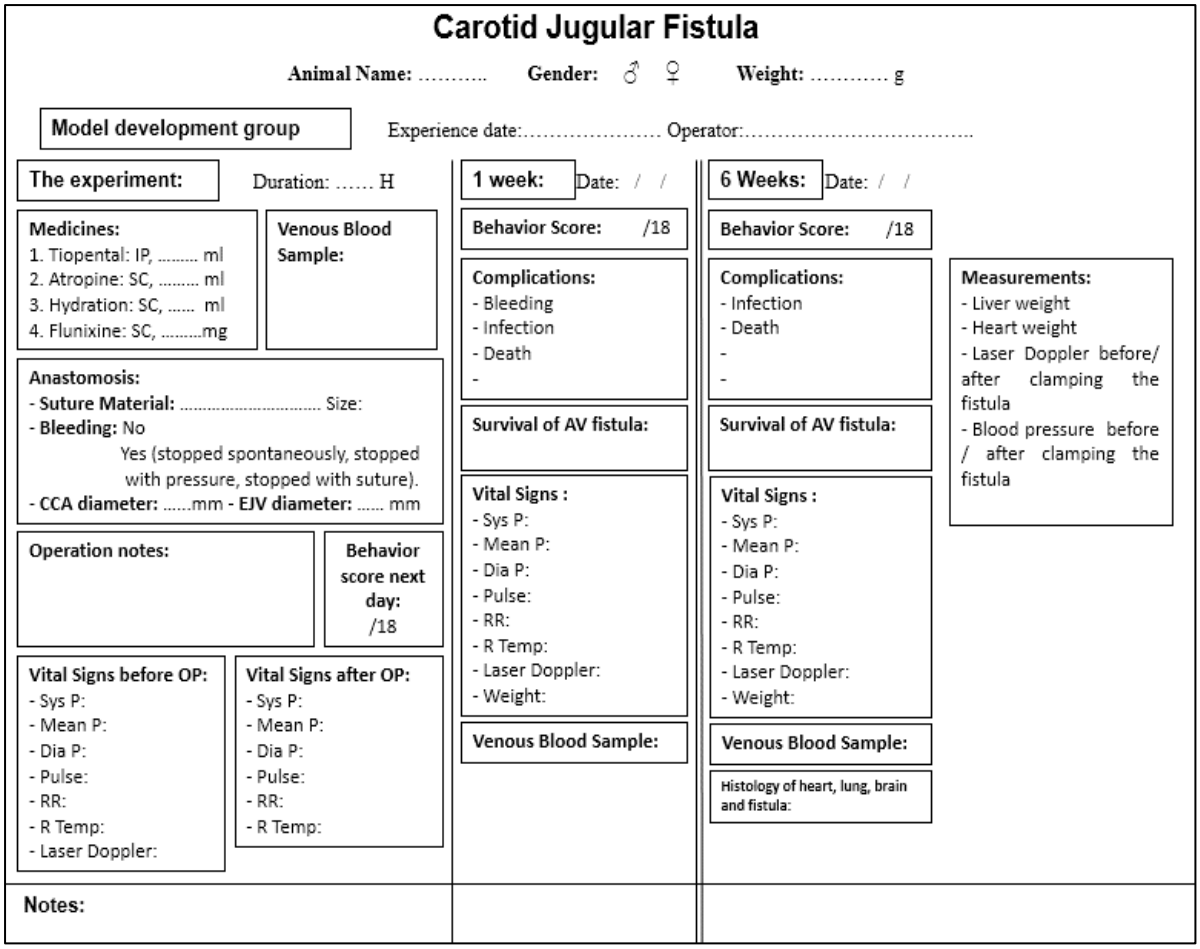

Figure 11. Documentation sheet for each

4. Results

4.1. General observations

Fifteen rats survived the period of follow-up (94%), one rat in FG died during the surgery because of uncontrolled bleeding after an accidental release of the temporary clip on the CCA. The vessels length was short in one rat, and it was necessary to cut the SCM to gain enough length for the anastomosis. Extensive sharp adventitial dissection of the EJV in another rat leaded to some difficulties in the construction of the anastomosis, and we had to cut the anastomosis and SCM to construct a new anastomosis. All the wounds were healed after less than one week without wound complications. No other surgical complications were noticed after the surgery as bleeding, aneurysm or infection.

4.2. Neurobehavioral assessment

Based on Garcia scale, the mean base neurological score was 17.33±0.82 for sham rats and 17.66±0.5 for fistula rats. The rats in both groups were revaluated after 6 weeks of the surgery by the same scale, and the mean neurological score was 17±0.89 for sham rats and 17.44±0.88 for fistula group. No significant differences were observed neither between the groups nor within the same group. However, this assessment showed some individual differences between the rats. The most important clinical sign in the neurological examination was the drop of the right upper eyelid in about half of the cases, 4 cases in FG and in 3 cases in SG.

4.3. Evaluation the patency of the fistula

The patency of all AVFs direct after surgery was checked by the physical examination using milking test which mentioned in the methods above. After one week of surgery, the fistula appeared as a subcutaneous small blue pulsatile mass in eight cases, 89% of the cases, and this sign was considered a sign of fistula patency. The patency of AVFs was also confirmed

using handheld Doppler in the form of high-frequency Murmurs. In the last stage of the study, the patency of the fistula was confirmed in all cases with the physical examination after the isolation of the fistula through a new surgical incision (see Figure 12).

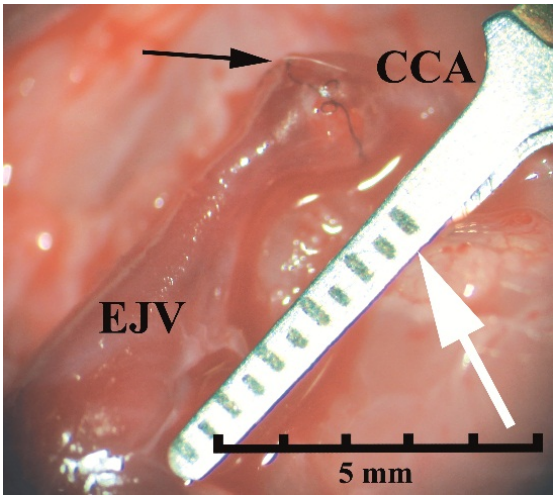

Figure 12. Surgical isolation of the carotid-jugular fistula at 6th week follow-up. Black arrow, anastomosis line. White arrow, 5 mm scale. CCA, common carotid artery. EJV, external jugular vein.

4.4. Laser Doppler measurements

The microcirculation of the liver and the right kidney was assessed six weeks after the surgery in both groups, this assessment was repeated after the acute occlusion of either the arterial limb of the fistula in FG or the CCA in SG. The liver BFU values were significantly lower ($p=0.01$) in FG (8.78±3.16) in comparison with SG (14.44±3.76), see Figure 13. However, these values increased significantly once again after the acute occlusion of the fistula ($P<0.01$) to reach this value 18.37±6.46, as shown in Figure 14.

As opposed to the liver, no significant difference of the kidney BFU values was observed between FG (21.73±4.49) and SG (17.52±4.56), and the kidney BFU values increased after the acute occlusion of the fistula to this value 26.08±3.71 but without reaching the significant level.

Table 3. Microcirculatory blood flux units (BFU) values of the liver and right kidney before and after the occlusion of the carotid artery and fistula in SG and FG, respectively.

Location	Sham group – 6 weeks after surgery		Fistula group - 6 weeks after AVF	
	Before occlusion[a]	After occlusion[a]	Before occlusion[b]	After occlusion[b]
Liver	14.44±3.76	15.08±4.45	8.78±3.16*	18.37±6.46#
Kidney	17.52±4.56	15.11±2.57	21.73±4.49	26.08±3.71

means±SD; FG: fistula group. SG: sham group. * p<0.05 vs. SG. # p<0.01 vs. FG before AVF occlusion. a: acute occlusion of the carotid artery. b: acute occlusion of the arterial limb of the fistula.

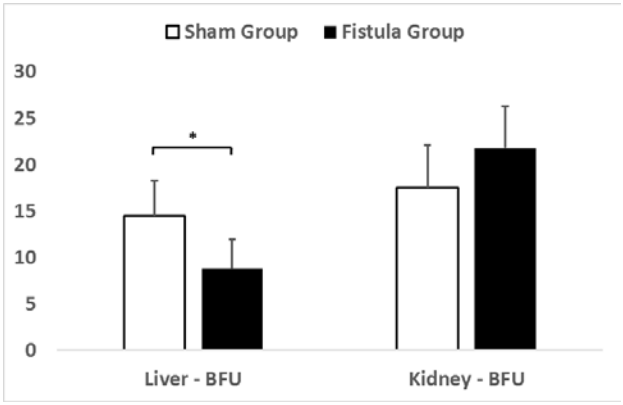

Figure 13. Significant decrease of liver BFU (Blood flux Units) in fistula group versus sham group. means± S.D. * p<0.05 vs. Sham Group

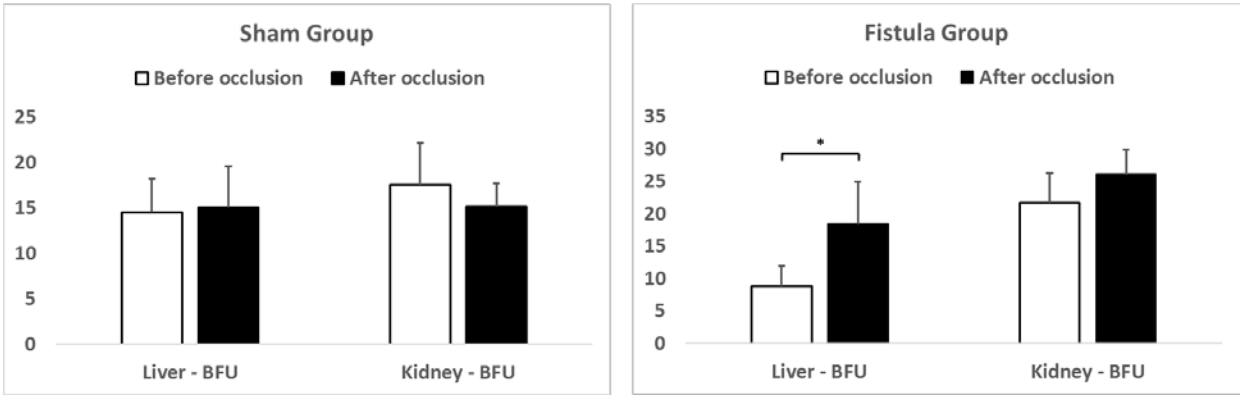

Figure 14. Significant increase of liver BFU (Blood flux Units) after the occlusion of the fistula. means± S.D. * p<0.01 vs. FG before AVF occlusion

The BFU units of both kidney and liver didn´t change significantly after the occlusion of the CCA in SG. Table 3 shows the results of the microcirculation assessment of the liver and right kidney using the laser Doppler, before and after the acute occlusion of the fistula and CCA in FG and SG, respectively.

4.5. Hemodynamic measurements

The results of hemodynamic measurements are summarized in Table 4. In non-invasive measurements, the baseline value of SBP in FG was 107.83±33.25 mmHg and significantly decreased ($p=0.041$) to 76.83±8.64 mmHg one week after the construction of the fistula. The invasive measurements showed also significant decrease ($p<0.01$) in SBP in FG (107.02±27.52 mmHg) in comparison with SG (145.17±13.09 mm Hg); The DBP is also significantly decreased ($p<0.01$) in FG (70.39±24.06 mmHg) in comparison with SG (117.59±13.72 mmHg).

Table 4. The hemodynamic measurements in the current study.

Non-invasive measurements	**Sham Group**		**Fistula Group**	
	Baseline (before surgery)	**1 week after surgery**	**Baseline (before AVF)**	**1 week after AVF**
HR (min-1)	395.17±14.20	409.17±28.39	402.5±29.12	345.67±20.91*
SBP (mmHg)	108.33±11.69	106.67±17.80	107.83±33.25	76.83±8.64*

Invasive measurements	**Sham Group - 6 weeks after surgery**		**Fistula Group - 6 weeks after AVF**	
	Before occlusion[a]	**After occlusion[a]**	**Before occlusion[b]**	**After occlusion[b]**
HR (min-1)	362.11±52.78	363.17±50.83	297.05±54.99	291.86±55.1
SBP (mmHg)	145.17±13.09	146.32±17.50	107.02±27.52#	118.65±26.62+
DBP (mmHg)	117.59±13.72	117.96±17.98	70.39±24.06#	94.58±23.06+

means±SD; AVF: arteriovenous fistula. SG: sham group. FG: fistula group. a: acute occlusion of the carotid artery. b: acute occlusion of the arterial limb of the fistula. * $p<0.05$ vs. FG baseline and $p<0.01$ vs. SG 1 week after surgery. # $p<0.01$ vs SG before occlusion. + $p<0.01$ vs. FG before occlusion.

The non-invasive measurements showed that HR in FG was 345.67±20.91 min^{-1} one week after the construction of the fistula and this value was significantly lower (p=0.026) in comparison with the baseline value 402.5±29.12 min^{-1}. The invasive measurement showed also marked decrease of the HR in FG in comparison with SG without reaching the significant level.

As a conclusion, we could appreciate significant decrease in SBP and HR by using both invasive and non-invasive measurements.

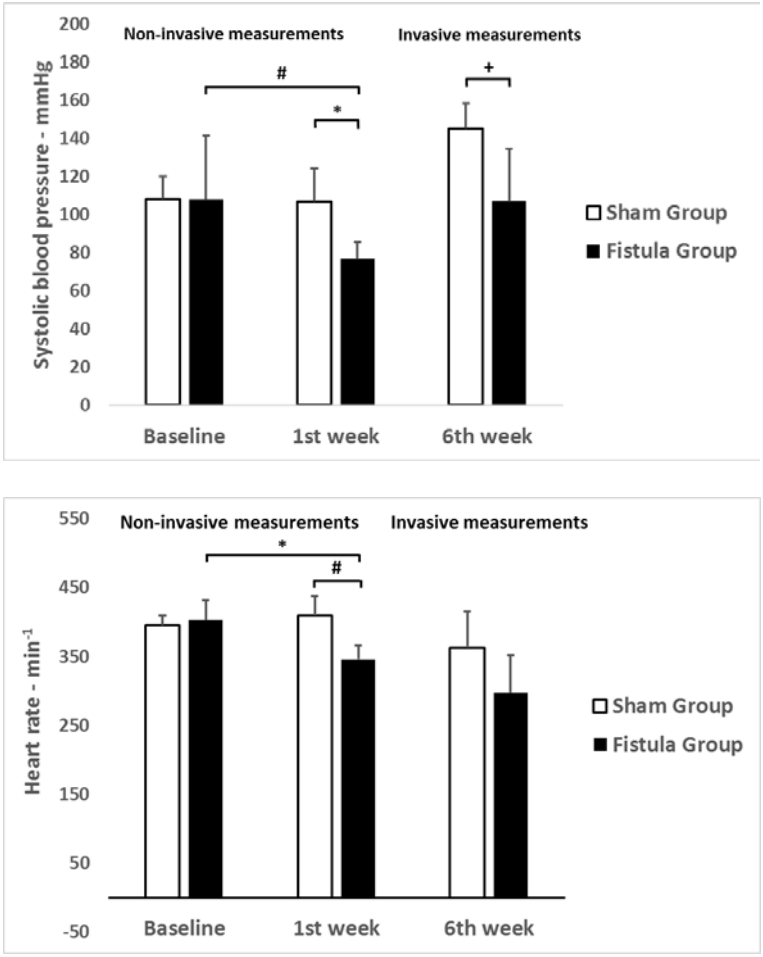

Figure 15. Significant decrease of systolic blood pressure and heart rate in fistula group versus sham group. means± S.D. * p<0.05 vs. FG – base, # p<0.01 vs. SG - 1st W, + p<0.01 vs. Sham Group – 6th W

The hemodynamic status changed significantly after the acute occlusion of the AVF. The invasive measurements showed immediate and significant increase in SBP (p<0.01) after the acute occlusion of the fistula, since the value of SBP before the occlusion was 107.02±27.52 mmHg and then value significantly increased after the occlusion to reach 118.65±26.62 mmHg.

The DBP increased also significantly ($p<0.01$) from 70.39±24.06 mmHg before the occlusion to 94.58±23.06 mmHg after the occlusion. Figure 16 shows the recordings of blood pressure and laser Doppler for the right kidney and liver in FG rats before and after the occlusion.

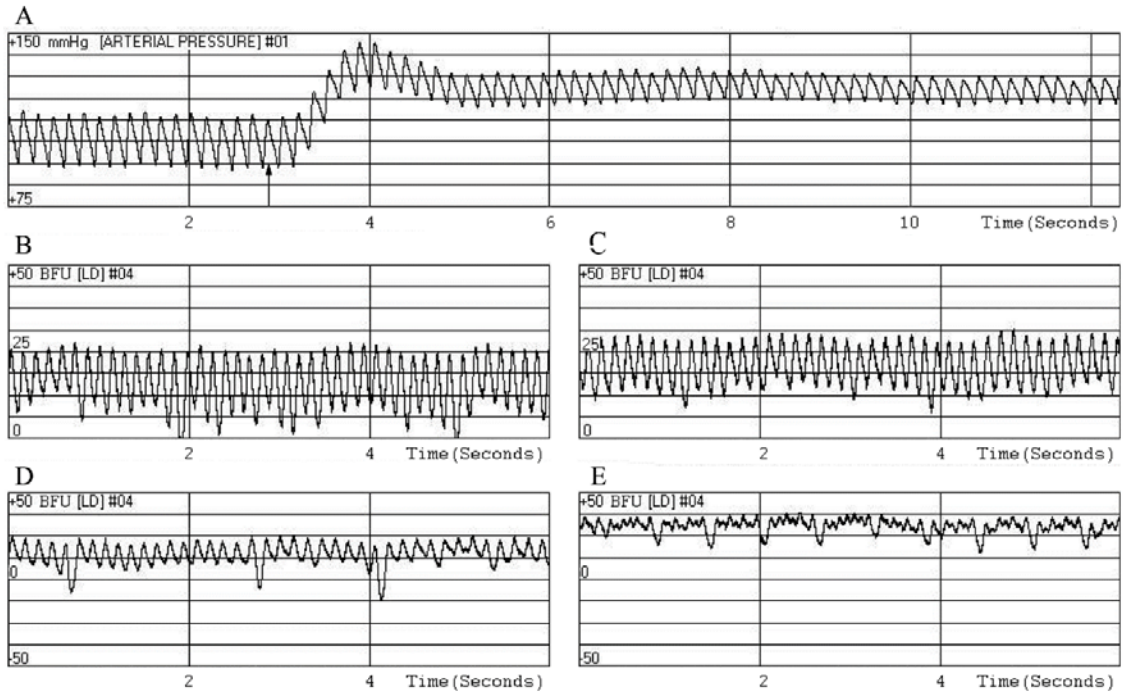

Figure 16. Continues recording of blood pressure during the acute occlusion of the AVF (arrow) shows a sudden increase of blood pressure (**A**). Laser Doppler recordings of the right kidney (**B and C)** and the liver (**D and E) (before and after** the acute occlusion of the fistula). BFU, blood flux units.

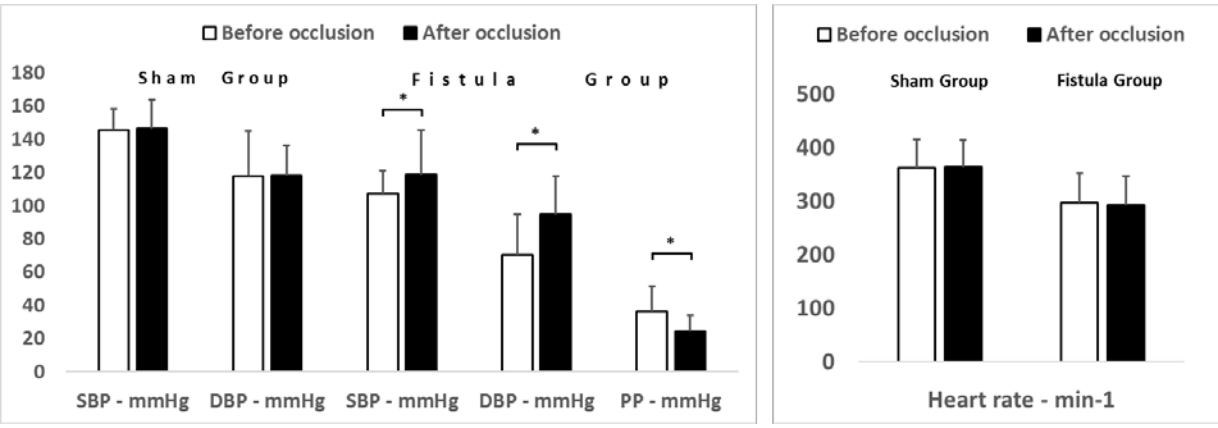

Figure 17. Significant hemodynamic changes after the occlusion of the fistula.

means± S.D. * $p<0.01$ vs. before occlusion

SBP: systolic blood pressure. DBP: diastolic blood pressure. PP: pulse pressure

No difference was observed in the HR after the occlusion in both groups. Pulse pressure (the difference between SBP and DBP) decreased significantly ($p<0.01$) from 36.36±15.06 mmHg to 24.07±10.63 mmHg after the acute occlusion of the fistula. The measured values in the SG did not differ significantly after the acute occlusion of the CCA.

4.6. Hematological measurements

Selected hematological results are shown in Figure 18. First, the groups were compared at each stage. No significant differences were observed in the baseline measurements between the groups except in the value of Hct and Plt count.

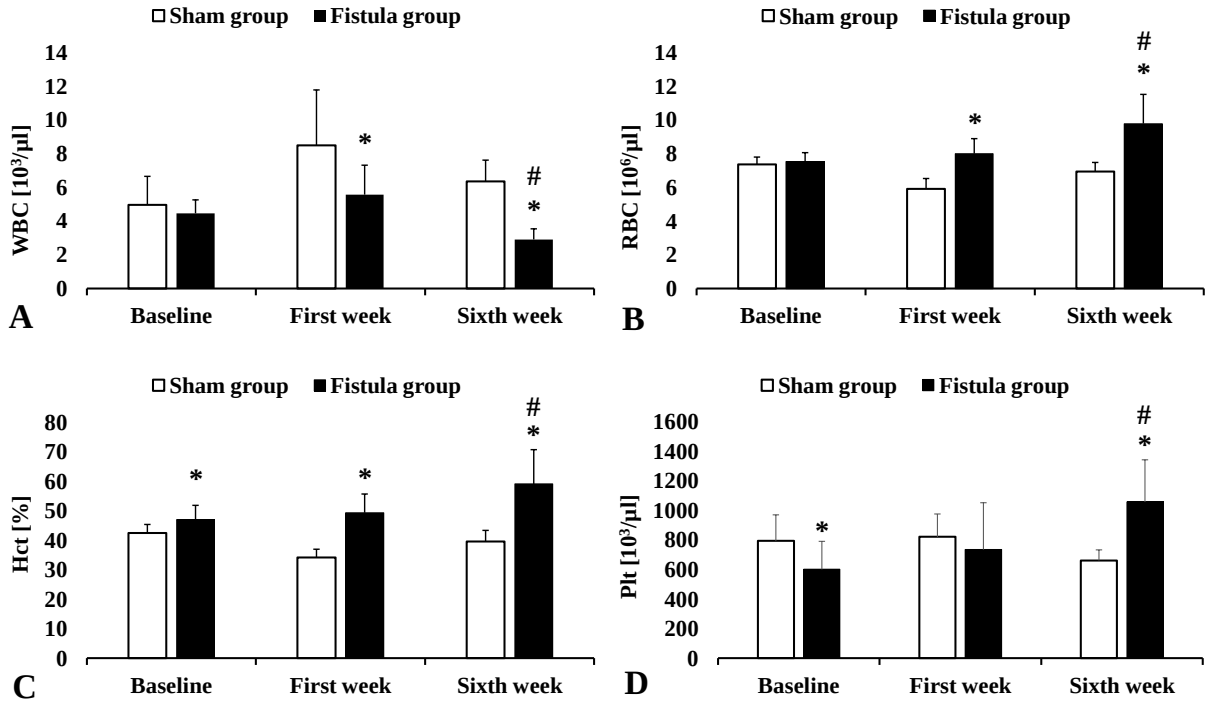

Figure 18. Selected hematological parameters in the sham-operated (n=6) and the fistula group (n=8) before surgery (base) and on the 1st and 6th postoperative weeks. A: white blood cell count (WBC), B: red blood cell count (RBC), C: hematocrit (Hct) and D: platelet count (Plt). means±S.D.; * $p<0.01$ SG at the same stage, # $p<0.01$ vs. FG-base.

In FG, a gradual increase was observed during the follow-up period in RBC count, Hct and Plt count, and these increases became highly significant ($p<0.01$) in FG-6W in comparison with SG-6W. WBC count increased temporarily in both groups 1 week after the surgery, but

the values of WBC counts were significantly ($p<0.01$) lower in FG-1W and FG-6W in comparison with SG-1W and SG-6W, respectively.

Second, in comparison with baseline measurements (FG-base), the parameters of RBC mass, RBC count ($p<0.001$) and Hct ($p<0.001$), were increased significantly in FG-6W measurements. RBC indices showed also hypochromic RBCs and wider distribution in RBC size in FG-6W in comparison with FG-base, as MCH decreased significantly ($p=0.002$) from 15.8±0.7 in FG-base to 13±2.2 in FG-6W and RDW-CV increased significantly ($p=0.007$) from 13.09±0.54 in FG-base to 13.76±0.7 in FG-6W.

Table 5. Hematological profile of sham and fistula groups.

	SG-base	FG-base	SG-1W	FG-1W	SG-6W	FG-6W	CG
WBC (10^3/µl)	5.0±1.7	4.5±0.1	8.5±3.3	5.6±1.8	6.4±1.3	2.9±0.6	4.3±2.7
RBC (10^6/µl)	7.4±0.4	7.5±0.5	5.9±0.6	8.0±0.9	6.9±0.5	9.8±1.7	7.9±1.2
Hgb (g/dl)	13.9±0.9	11.9±1.1	11.5±2.8	11.6±0.7	13.2±1.2	12.5±1.2	11.8±1.5
Hct (%)	42.4±2.9	47.0±4.8	34.2±2.8	49.3±6.4	39.5±3.8	59.0±11.6	47.1±6.2
MCV (fl)	57.2±1.3	62.2±3.9	57.9±2.5	61.6±2.7	56.9±1.4	60.2±1.8	59.7±2.3
MCH (p g)	18.8±0.6	15.8±0.7	19.5±0.8	14.6±1.4	19.1±0.6	13.0±2.2	14.9±1.0
MCHC (g/dl)	32.9±0.7	25.5±1.4	33.6±0.7	23.8±2.8	33.5±0.7	21.7±3.9	25.0±1.3
Plt (10^3/µl)	795±176	601±190	821±155	735±317	662±72	1058±286	846±171

means±SD. CG: control group, n=6. FG: fistula group, n=8

1W and 6W: first and sixth week after the construction of the fistula

4.7. Red blood cell deformability

The following two parameters, $SS_{1/2}$ and $EI_{max}/SS_{1/2}$, were used to compare the EI-SS patterns inter- and intragroup. These two parameters were calculated from the EI-SS curves, and figure 19 shows a comparison of the values of these two parameters. No significant difference in baseline values of these two parameters was observed between the two study groups, but they changed significantly in FG during the follow-up period.

The $EI_{max}/SS_{1/2}$ was significantly lower in FG at 1 week (FG-1W, p=0.025) and 6 weeks (FG-6W, p=0.039) after establishment of the fistula compared to parallel values from the SG (SG-1W and SG-6W). While the $SS_{1/2}$ value was significantly higher in FG at 1 week (FG-1W, p=0.003) and 6 weeks (FG-6W, p=0.043) after establishment of the fistula compared to parallel values from the SG (SG-1W and SG-6W).

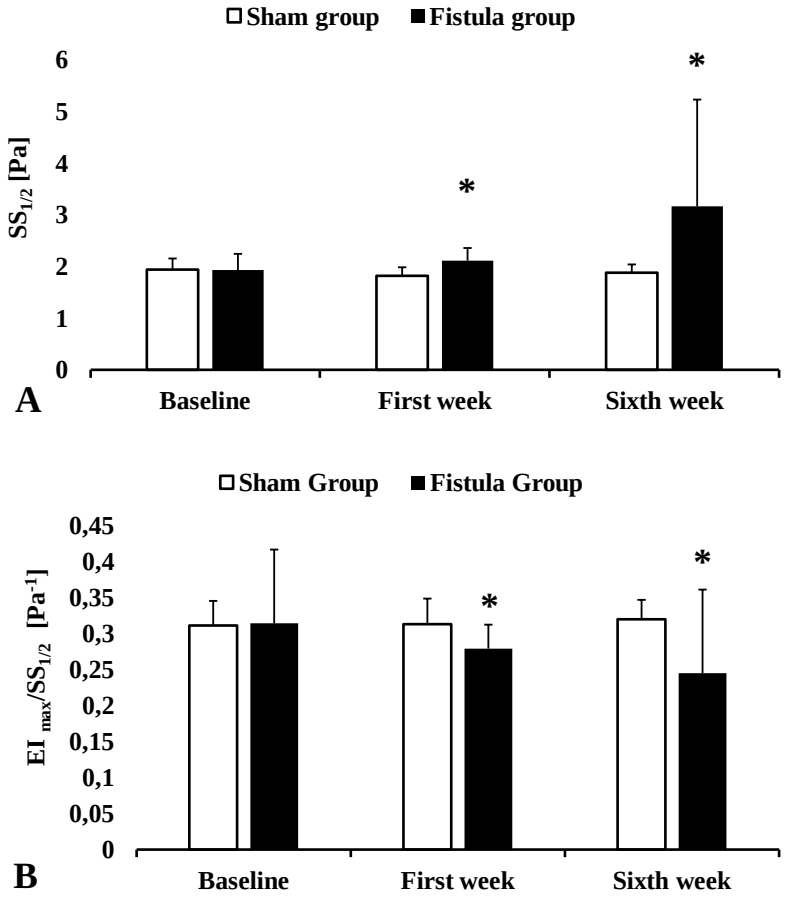

Figure 19. Red blood cell deformability describing parameters in the sham-operated (n=6) and the fistula group (n=7) before surgery (base) and on the 1st and 6th postoperative weeks. A: shear stress at half-maximal elongation index ($SS_{1/2}$), B: ratio of maximal elongation index (EI_{max}) and $SS_{1/2}$. means±SD; * p<0.05 vs. SG.

4.8. Red blood cells membrane stability

Figure 20 shows lower RBC deformability profile in FG-6W both before and after membrane stability test and Table 6 shows the changes of the parameters of RBC deformability before and after the membrane stability test.

After applying membrane stability test (100 Pa shear stress for 300 s) on RBCs, the deformability of RBCs was decreased significantly ($p<0.01$) in SG-6W for shear stress range (0.95-30 Pa) and in FG-6W for shear stress range (3-30 Pa). The ratio of RBC deformability values after/before applying the stress was calculated at each shear stress and compared between FG-6W and SG-6W. This ratio was smaller in FG-6W, however, without significant differences**.**

Table 6. Changes of $EI_{max}/SS_{1/2}$ and $SS_{1/2}$ values before and after applying mechanical stress on the samples (100 Pa for 300 s) sixth week (6W) after the surgery.

	FG-6W		**SG-6W**	
	before	**after**	**before**	**after**
$EI_{max}/SS_{1/2}$ [Pa^{-1}]	0.27±0.11	0.13±0.05*	0.32±0.05	0.22±0.04#
$SS_{1/2}$ [Pa]	2.75±1.66	4.66±1.94*	1.90±0.29	2.69±0.45#

means±SD; SG: sham group, *n*=6. FG: fistula group, *n*=8

* p value <0.01 vs. before. # p value <0.05 vs. before.

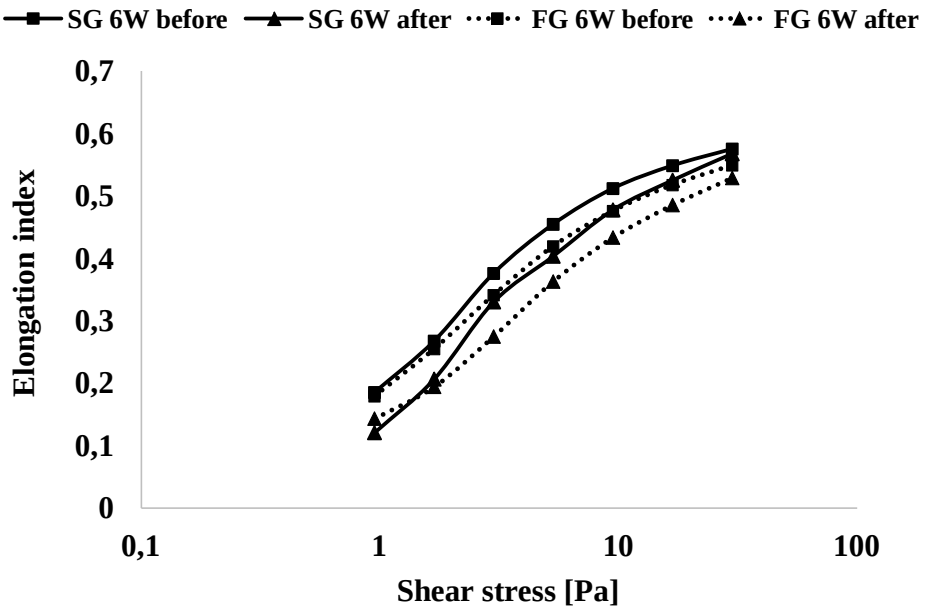

Figure 20. Elongation index – shear stress curves of RBC deformability before and after applying mechanical shear stress (100 Pa for 300 s). Means±S.D.; SG: sham group, n=6. FG: fistula group, n=8
6W: sixth week after the surgery

4.9. Comparing young and old RBCs deformability

After the separation of the subpopulations of RBCs, no significant differences were observed in hematological parameters except significant increase (p=0.014) of RDW-CV in the bottom 10% of FG-6W in comparison with the top 10% of FG-6W. Figure 21 shows EI-SS curves to compare the deformability of two RBC subpopulations, top 10% RBCs showed slightly higher deformability than bottom 10% RBCs without significant differences between the subpopulations.

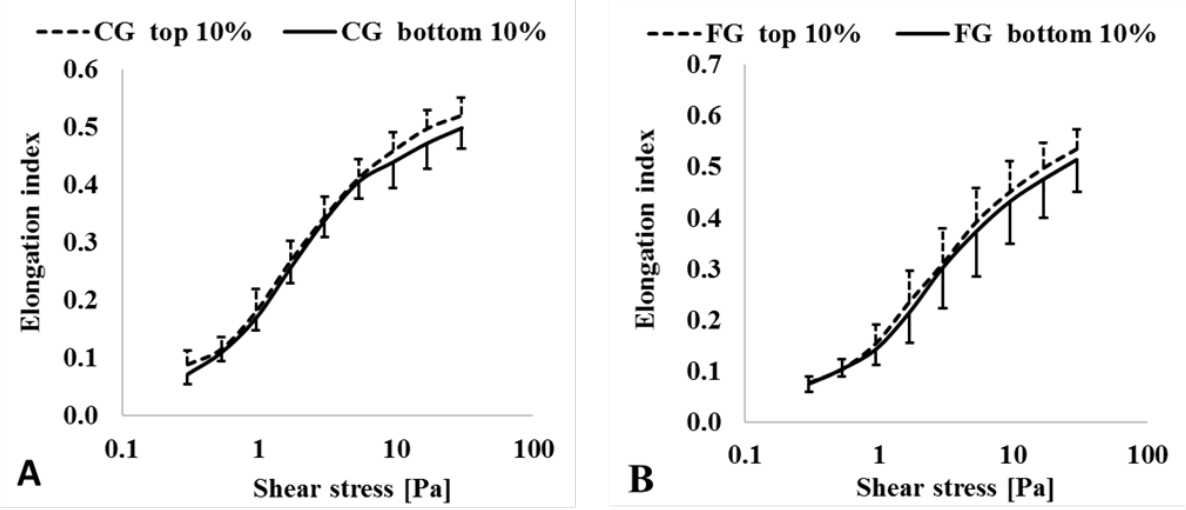

Figure 21. Elongation index – shear stress curves of the 'young' (top 10%) and 'old' (bottom 10%) RBCs in fistula group (A) and in control group (B). Means±S.D.; CG: control group, FG: fistula group. Bottom 10% and top 10% of the RBC column in centrifuged samples, considered as dominantly 'old' or 'young' RBCs, respectively.

4.10. The effects of hematocrit standardization

There was a significant difference in hematocrit values between the CG and the FG, where the Hct in the CG was 47.1% and in the FG in the sixth week measurements 59.0% (see Table 5).

The two calculated parameters ($EI_{max}/SS_{1/2}$ and $SS_{1/2}$) did not show statistically significant changes in the CG after hematocrit standardization, while these two parameters

changed significantly after hematocrit standardization in the FG, as the $EI_{max}/SS_{1/2}$ increased and the $SS_{1/2}$ decreased significantly after the decrease of Hematocrit (see Table 7).

Table 7. Selected variables comparing properties of RBC subpopulations after adjusting the sample hematocrit.

Group	Variable	Native sample	Sample with adjusted Hct for 40%	
			'Bottom'	'Top'
CG	$EI_{max}/SS_{1/2}$ [Pa^{-1}]	0.3±0.04	0.28±0.04	0.28±0.06
	$SS_{1/2}$ [Pa]	1.93±0.19	1.84±0.28	1.99±0.39
	RDW-CV%	13.6±0.36	13.2±0.45*	13.49±0.51
FG-6W	$EI_{max}/SS_{1/2}$ [Pa^{-1}]	0.17±0.1	0.19±0.11*	0.22±0.11*
	$SS_{1/2}$ [Pa]	4.11±2.36	3.7±1.97	3.19±1.46*
	RDW-CV%	13.76±0.51	14.29±0.74*,#	13.34±0.61*

means±S.D.; CG: control group, *n*=6. FG-6W: fistula group, *n*=5. 6W: sixth week after the construction of the fistula. Bottom and top: bottom 10% and top 10% of the RBC column in centrifuged samples, considered as dominantly 'old' or 'young' RBCs, respectively. * $p<0.05$ vs. native Hct sample, # $p<0.05$ vs. FG-6W - Top.

4.11. The weight of body and organs

The mean body weight of SG rats was 267.17±11.18 g and they gained weight gradually to 287.5±15.45 g six weeks after the surgery, while the body weight of FG rats decreased slightly one week after the construction of the fistula and they regained the weight to 294.57±29.2 g at the end-point.

Table 8 shows the absolute and relative weights of the organs of FG and SG rats 6 weeks after the surgery. The mean absolute and relative weights of the hearts were increased significantly in FG compared with SG.

The effect of an arteriovenous fistula on the weight of the organs varies according to the size of the fistula, and the table (9) shows the relative heart and lung weight in different studies including ours arranged according to the size of the fistula.

Table 8. Absolute and relative weights of the organs of FG and SG rats 6 weeks after the surgery.

	SG		FG	
Body weight	287.5±15.45	g	294.67±29.2	g
Heart Weight	0.9±0.05	g	1.3±0.1*	g
HW/BW	3.15±0.24	mg/g	4.45±0.39*	mg/g
Liver Weight	8.25±0.75	g	8.54±1.58	g
LW/BW	28.45±1.72	mg/g	28.99±4.44	mg/g
Lung Weight	1.34±0.11	g	1.4±0.1	g
LuW/BW	4.66±0.38	mg/g	4.42±0.22	mg/g

means±SD; SG: sham group. FG: fistula group. *: $p<0.001$ vs. SG.

Table 9. The gradually increase of the relative weight of the heart and lung in proportion to the size of the fistula 4 weeks after the fistula construction.

The fistula diameter	**Control group**[109,110,*]		**1mm****	**1.2mm**[109]	**1,6mm**[110]**#**	**1.8mm**[109]
Type of fistula	No	No*	CJF	ACF	ACF	ACF
Strain	Wistar	CD outbred*	CD outbred	Wistar	Wistar	Wistar
Gender	male	Female*	Female	male	male	male
Heart weight / Body weight (mg/g)	3.9±0.1, 3.5±0.1	3.97±0.61*	4.38±0.39	4.9±0.1	6.6±0.2	6.6±0.3
Lung weight / Body weight (mg/g)	3.8±0.2, ~4.3±0.1	-	4.42±0.22	~4.73±0.1	7.3±0.6	~6.6±0.3

means ± SD; CG, control group. * current study. ** current study (the artery diameter was considered as the diameter of the fistula) (the measurements were after 6 weeks). # used needle was 16G (i.e. the outer diameter is 1.615mm). CJF, Carotid-Jugular Fistula. ACV, aortocaval Fistula. ~ Calculated from the study values. -, no measurements.

4.12. Histological examinations

Figure 22 shows the histological examination of the vessels and hearts from the fistula group and the sham group.

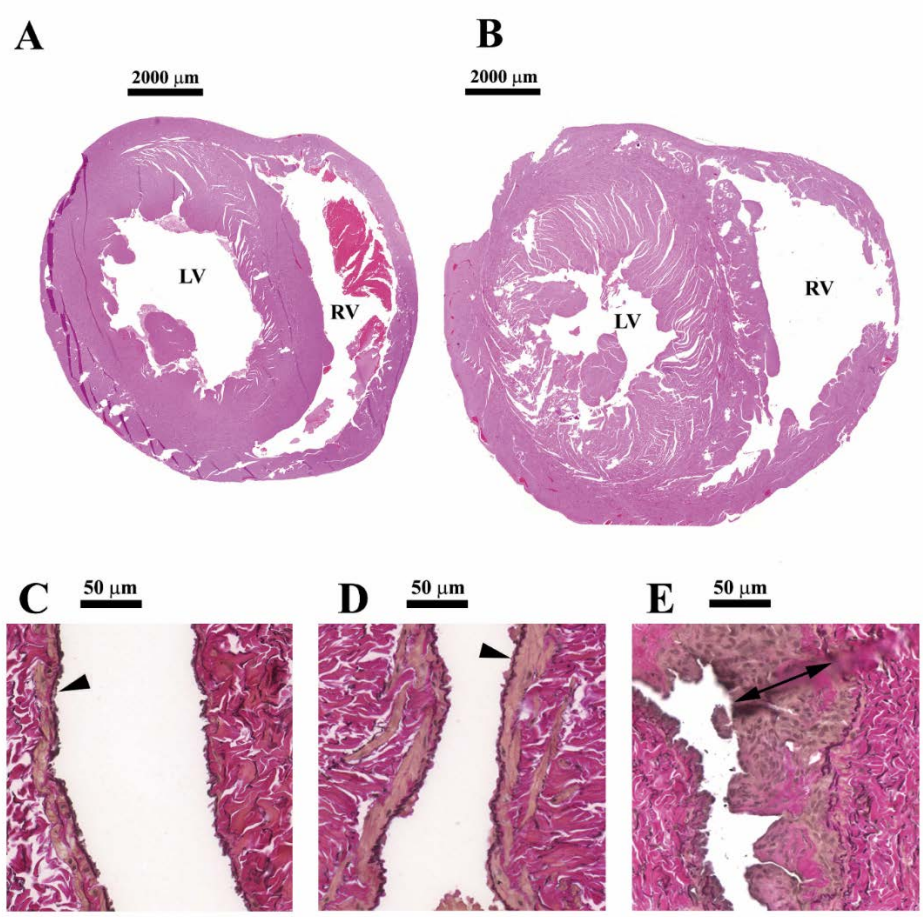

Figure 23. Histological examination of the hearts and vessels from fistula group (FG) and sham group (SG), 6 weeks after the surgery. Heart sections from SG (**A**) and FG (**B**) showed a significant increase in left ventricular wall thickness. LV: left ventricular. RV: right ventricular. These sections were stained with H&E. Scale bar: 2000 µm. Original magnification: x200. (**C, D and E**) compare the histological findings of the vein in SG (**C**) with non-operated vein in FG (**D**) and with venous limb of fistula in FG **(E)**, these findings showed significant intima hyperplasia in (**E**). Arrowhead: intima. Double headed arrow: the thickness of fistula intima. These sections were stained with elastic Van Gieson. Scale bar: 50 µm. Original magnification: x600.

The measurements showed significant left ventricular hypertrophy (LVH) in FG since wall thickness values were increased significantly ($p=0.008$) in FG (3218±0.7 µm) in comparison with SG (2425±0.7 µm), but no significant difference was observed in right ventricular wall thickness between the groups. Intima proliferation was observed in the venous limb of the fistula and highly significant increase ($p<0.001$) in the thickness of the intima of the venous limb of the fistula (84.56±26.8 µm) was observed in comparison with non-operated EJV in FG (5.37±1.2 µm) and EJV in SG (3.8±0.69 µm).

5. Discussion

Arteriovenous fistula is the recommended vascular access for hemodialysis patients.[111] Many researches were conducted to evaluate the arteriovenous fistulas and their effects, but their effects on the microcirculation and the mechanism of these effects are still not well understood. Here we will discuss various factors affecting the microcirculation in cases of arteriovenous fistulas: hemodynamic changes, hematological and hemorheological parameters.

An arteriovenous fistula in the neck region, carotid-jugular fistula, was used in our study. There are several models in the medical literature of arteriovenous fistulas constructed under the microscope, and each has advantages and disadvantages in terms of technical difficulties, complications, and systemic effects. We will describe all these aspects according to our model.

Surgical Procedure

Hemodialysis arteriovenous fistulas are performed in humans by creating an anastomosis between a peripheral artery and a peripheral vein. It's mostly a side-to-end anastomosis, but it can be end-to-end or end-to-side. The creation of the anastomosis in the models is not limited to the suture technique or to the peripheral vessels, most models tend to have central AVFs using other techniques. It is because of various anatomical and technical reasons such as the small diameter of the peripheral vessels and the need for more time and effort to sew the anastomosis under the microscope. One of these techniques is the puncture technique, where two adjacent vessels (artery and vein) are punctured with a needle, creating a channel between these two vessels, and this channel remains open due to the pressure difference between the artery and vein.[112] There are several other techniques described in the medical literature to facilitate work with these small models, such as insertion of the artery into the vein or cuff technique, and various forms of anastomosis.[57,65,68,96,98]

We chose suturing technique to perform this anastomosis between two relatively large peripheral vessels, as our goal was to follow the rats for a relatively long time so a safe anastomosis with minimal complications was needed.

The two golden rules in creating the anastomosis under the microscope are to perform an anastomosis without any tension on the anastomosis line and to work in a moist environment.

Our technique is not complex and some technical tips and tricks should be mentioned. First, it is important to perform the surgery quickly and without vascular injuries, so we recommend cutting the subcutaneous tissue first medially until reaching the sternocleidomastoid muscle and then continuing the isolation laterally, where it is easy to find the external jugular vein under the salivary glands and cervical soft tissues. The Isolation of the common carotid artery can also be easily performed medial to the SCM, i.e. by slight retraction of the SCM laterally. Second, to reduce the risk of vascular injury, it should be mentioned that isolation of 10-12 mm from the CCA is enough to perform this anastomosis, and the isolation until the bifurcation is not necessary and may lead to uncontrolled bleeding when the bifurcation of CCA is injured. Third, the resection of the sternocleidomastoid muscle should not be done routinely, although it has been routinely performed in some studies.[57] There is enough place and length of both artery and vein to perform an anastomosis without the resection of the SCM, so we could avoid potential muscle bleeding after such procedure. The resection was performed for technical reasons in only two cases in this study. Fourth, it is important to avoid the extensive dissection of the venous adventitia as it makes the edge of the venous anastomosis difficult to distinguish and leads to a high rate of technical failure. Fifth, it is recommended that the anastomosis be tested for leakage with a normal saline solution, filling the surgical field with a transparent solution makes it easier to see the blood flow from the leakage under the microscope. Finally, a new incision was made about 1 cm higher than

the old incision at 6th week follow-up, in order to start the isolation from a non-scarred area and not to damage the fistula at this stage.

The superficial location of the CJF allowed us to examine the patency of the fistula without invasive interventions, in contrast to central arteriovenous fistulas, for which the patency of the fistula is difficult to examine by physical examination. This fistula appeared as a pulsating mass under the skin and it was easy to observe the pulse just by inspection. We also examined the fistula using a hand-held Doppler, the murmurs produced from the turbulent flow in the fistula were a sign of the patency of the fistula. However, it is not too simple to distinguish these sounds from the arterial sounds due to the high frequency heart rate. The location of a CJF simulates the superficial location of the hemodialysis arteriovenous fistulas in humans and provides a model for studies about local treatments or local measurements such as measuring local microcirculation, unlike the aortocaval fistula,[113] one of the most common types of fistula used in studies.

Complications and limitations

The number of animals used in the studies is limited according to animal protection laws. Therefore, we cannot talk about the statistical significance of surgical complications which occurred in individual cases. However, it is important to describe these complications to improve the working methods in our laboratories. Despite all the preventive measures followed in our study to reduce the risk of hemorrhage, one rat died of uncontrolled arterial hemorrhage. We have changed the surgical protocol after this case by using two temporary clips to control the artery instead of one.

Studies have reported different mortality rates ranging from 0 to 47%.[100,114–116] The mortality rate is expected to be higher in central arteriovenous fistulas where surgical trauma is greater and the risk of bleeding and concomitant infection is greater. Most of the deaths in

these studies occurred within 24-48 hours postoperative, and the cause of death was congestive heart failure or other unknown causes.[52,100,114]

No other surgical complications occurred in our study, as we did not observe any postoperative death or wound healing disorder. Some studies reported other complications, Langer et al. reported one case of septic thrombosis of the femoral fistula postoperatively.[116]

We know that all animal models have advantages and disadvantages, and our model here is not an exception. To create a fistula by puncture technique is a simple and fast procedure compared to suturing technique, but it is not possible to do it in the neck region since the internal carotid artery and the internal jugular vein are not adjacent as in the case of the aorta and caudal vena cava. Other methods have been used to perform anastomoses in studies, which may shorten the time of the surgical intervention and the surgical trauma, however we wanted to perform a safe anastomosis and most of the surgical interventions in our study were done within less than 45 minutes. The diameter of the CJF is smaller than the diameter of the ACF,[109] thus the expected hemodynamic effect is relatively less. However, the diameter of the jugular carotid fistula is greater than that of other fistulas in the femoral or saphenous vessels.

Neurobehavioral Assessment

Neurological evaluation using the Garcia scale showed that no significant neurological deficit occurred in both groups. This supports the medical literature that unilateral carotid artery ligation in rats does not cause significant neurological deficit, unlike the case in humans with carotid artery ligation.

The dropping of the right upper eyelid (the same side of the surgery) occurred in approximately half of the rats in both study groups, and this drop (so-called ptosis) was interpreted as part of Horner's syndrome especially it happened in both FG and SG rats. Horner's syndrome is a well-known syndrome after carotid artery surgery in both humans and

rats, and it consists of three components: ptosis, miosis (a constricted pupil) and enophthalmos (posterior displacement of the eyeball within the orbit). This syndrome is caused by disruption of the oculosympathetic system, and one of the pathways of this system (superior cervical ganglion) is located dorsally to the carotid bifurcation.[117]

Hemodynamic changes

From our point of view, it is important to prove the hemodynamic effect of an arteriovenous fistula in each AVF model before performing other various measurements, since this hemodynamic effect is an indirect evidence of the fistula patency, and it is also evidence of the hemodynamic significance of the fistula.[118]

Most studies agree that a significant decrease in mean blood pressure (MAP) occurred after the creation of the fistula,[55,56,110,119] and that a significant cardiac hypertrophy developed within 4 weeks with near-normal function.[56,119]

The CJF model in our study showed expected hemodynamic effects by both non-invasive measurements at the beginning of the study and invasive measurements at the end of the study. The non-invasive measurements showed a statistically significant decrease in SBP at 1st week follow-up in comparison to baseline measurements, and the invasive measurements showed a statistically significant decrease in both SBP and DBP in FG compared to SG (see Table 4).

We noticed the heterogeneity of the data between the invasive and non-invasive measurement methods in SG. Therefore, no data comparison was done between the two methods, and we only compared the results within the same method. We only used the SBP from the non-invasive methods data, as these methods are not so sensitive to measure DBP. However, the invasive methods remain the most accurate methods and show the actual changes

in the hemodynamic parameters, but we did not do it at the beginning of the study as they may have affected the course of the study.

Arteriovenous fistula leads to an increase in cardiac output in humans by various mechanisms, including an increase in the heat rate. On the contrary, rat experiments showed that the increase in cardiac output does not depend on the increase in heart rate, as the pulse decreased or remained unchanged after the creation of the fistula.[114,120,121] We observed similar results in our study as the heat rate decreased after the construction of the fistula, by both invasive and non-invasive measurements.[120] The mechanisms of increasing cardiac output in rats may be different from those in humans and depend on the decrease in the heart rate to allow the heart to get sufficient venous return between the two heartbeats since the heart rate in rats is very fast compared to humans and is normally 300-400 beats per minute. However, the question remains open about the underlying physiological mechanisms behind it and needs more detailed hemodynamic studies to answer it.

One of the methods to assess the hemodynamic significance of the arteriovenous fistula is to evaluate the hemodynamic changes after acute occlusion of the fistula.[122] Therefore, we decided to study these changes at the 6th week measurements using invasive methods since they measure the hemodynamic parameters in real time. Hemodynamic changes after the acute occlusion of the fistula in humans are known as Nicoladoni or Branham sign, which is a sudden drop in the heart rate, a rise in blood pressure, and a decrease in pulse pressure.[3,122] Our study showed a sharp increase in both systolic and diastolic pressures after acute closure of the fistula, due to several physiological mechanisms, including the sharp rise in peripheral vascular resistance. The heart rate did not change significantly after the acute fistula occlusion, and this may be due to the effect of atropine given preoperatively. However, the statistically significant changes in both systolic and diastolic pressure after occlusion of the fistula confirm the hemodynamic importance of this type of fistula.

Liver and Kidney Microcirculation

According to our information, there is a lack of studies evaluating the microcirculation in the tissues and organs distal to the fistula. In our study, we aimed to evaluate the effect of arteriovenous fistulas on the microcirculation as well as to provide an animal model for conducting such studies. The measurements were done in our study using the laser Doppler, and the microcirculation of the liver and the kidney were evaluated as distal organs, since the fistula in our model is located on one of the main aortic arch arteries proximal the origin of the renal arteries and the hepatic artery. The hepatic microcirculation showed results comparable to the hemodynamic results, where the values of liver BFU were statistically significantly lower in the FG compared to the SG, and then these values increased significantly after the acute occlusion of the fistula. The renal microcirculation did not show significant changes in the values of these parameters, neither between the two study groups nor after the acute occlusion of the fistula, despite the important hemodynamic changes. These results refer to the ability of the kidney to self-regulate the local blood flow.

The increase in liver BFU after the acute fistula occlusion confirms the functional significance of this fistula and emphasizes the role of fistula binding or ligation in the management of fistula-related ischemia. These results also confirm that the hemodynamic changes and steal syndrome play the most important role in microcirculation impairment since the arteriovenous fistula steal flow from the distal organs.

Hematology

The effects of arteriovenous fistula on RBCs are not yet total understood, although the structure and function of red blood cells play a significant role in the blood physiology, and this study came in attempt to understand more about the changes of RBCs properties in the presence of AVF.

Our results showed a significant increase in the red blood cell count and hematocrit in the first- and sixth-week measurements of the fistula group compared to the parallel measurements in the sham group. There was no significant difference in the basal RBC count between the two study groups, but there was a statistically significant difference in the basal hematocrit between the two study groups, but we could notice from figure 18 that this difference has steadily increased over time, which confirms the significant effect of fistula on hematocrit.

We have interpreted the increased measured erythrocyte mass in fistula rats due to secondary polycythemia induced by excess erythropoietin in the blood.[42] As known, Erythropoietin secretion is regulated as a reactive process to tissue hypoxia mediated by factors called hypoxia-inducible factors (HIF). These are transcription factors of the erythropoietin gene and have other effects, such as promoting angiogenesis.[42,123,124] Tissues hypoxia in the case of the AVF occurs systemically due to accompanying heart failure, or in distal organs due to steal syndrome,[38,125] or locally in the venous segment of the fistula due to the damage of the vasa vasorum.[22,27,126]

Studies have not shown conflicting results about the effect of arteriovenous fistula on hematocrit values, as some studies showed a significant decrease in the hematocrit value using an aortocaval model,[119,127] while another study showed no effect of a saphenous arteriovenous fistula on the hematocrit value.[52] However, our results have shown significant increase in hematocrit in FG. The location of the arteriovenous fistula may play a role in interpreting these results, as the liver and the kidney are the distal organs in our model, and they are both the most important producers of erythropoietin in the body, while in the case of aortocaval model and saphenous model, the distal organs are usually the lower extremities and the pelvic organs.[123,128]

Polycythemia is a reaction of hypoxia and shows individual differences between organisms, as it occurs in some cases of hypoxia while it may be absent in others without an apparent cause.[42,129] Upon re-evaluating our results individually, we found that the hematocrit increased in all rats in the fistula group, but the increase ranged from a slight increase in some cases to a large increase in other cases.

Comparison of other measured blood parameters showed indirect signs of iron deficiency, such as an increase in the red blood cell distribution width (RDW), a decrease in mean corpuscular hemoglobin (MCH), and an increase in the platelet count (plt). We did not determine the serum iron levels in our experiment because it was not included in the study protocol at the beginning. The assumed iron deficiency is secondary finding that we would mention, especially since polycythemia is associated in a third of cases with iron deficiency due to depletion of iron stores to support erythropoiesis.[42] Although the HIFs promote iron intake in the intestine, iron deficiency in commercially used food and chronic intravascular hemolysis by AVF leads to a further decrease in iron stores.

The platelet count increased gradually during follow-up in the fistula group, while the mean platelet volume (MPV) decreased. These changes could be interpreted as an accompanied iron deficiency, but there are other differential diagnoses for thrombocytopenia in this case such as acute phase reactions and spurious increase related to fragmented RBCs.[130–133]

Several studies have focused on the red blood cell distribution width (RDW) as a risk factor for arteriovenous fistula failure, heart failure, and cerebral vascular disease.[25,134–137] From a hemorheological point of view, studies showed an association between an RDW value greater than 14% and a reduction in RBC deformability.[138–140] The RDW value increased in fistula rats significantly after 6 weeks of creation of the fistula compared to the basal values in our study, and the RDW value in the old RBCs was statistically significantly higher than the RDW value in the young RBCs. Through further comparison of these results with the

hemorological results, it can be noted that the increase in RDW was accompanied by a decrease in RBC deformability as well.

Hemorheology

The RBC deformability is compared by comparing the (Elongation index / shear stress) charts, and to simplify this comparison process we compare two parameters calculated from these charts: $SS_{1/2}$ and the ratio between EI_{max} and $SS_{1/2}$. A higher $SS_{1/2}$ value indicates that more force is required to reach the half-maximal elongation, i.e. the ability of the RBCs to alter their shape (deformability) is impaired. A lower $EI_{max}/SS_{1/2}$ ratio also refers to a reduced RBCs deformability. The overall evaluation of the rheological parameters showed a statistically significant decrease in the RBCs deformability in FG compared to the SG in both the first and sixth week measurements.

The individual evaluation of the RBCs deformability parameters showed a significant difference between the FG rats, as some rats did not show a significant change in the RBCs deformability parameters, while others showed significant drop in these parameters. These large individual differences occurred even though all of these rats were of the same gender, strain, and age and had the same experimental environment. These individual differences explain the high value of SD.

Density separation of RBC subpopulations

Rheological measurements for clinical applications are usually performed on the total blood sample and give an impression of the rheological behavior of a large population of cells. In research applications, separating red blood cells into sub-populations based on their density, for example, increases the amount of information that can be obtained in these studies and provides us with RBC deformability distribution histogram in the sample.[47,141]

Our idea was that the arteriovenous fistula affects the lifespan of the red blood cells, as it leads to the elimination of a large number of weak, old red blood cells through the high mechanical stress inside the fistula, and thus the red blood cells in the fistula group are mostly young and there is no wide difference in the rheological parameters between the subpopulations. Whereas the red blood cells in the control group contain all the spectra of the red blood cells, old and young, so we will see a wide difference in the rheological parameters. In other words, we intended to study the RBC deformability distribution.

The subpopulations of RBCs were separated using centrifugation at 1800 × g for 1 hour. Young RBCs showed better deformability than those measured in adult RBCs in both groups, but the expected difference in subpopulations behavior did not appear between the two study groups, CG and FG. Maybe we had to centrifuge using higher forces or longer time as in other studies (10000 × g for 15 min).[47]

Hematocrit standardization

The measured parameters ($SS_{1/2}$ and $EI_{max}/SS_{1/2}$) in the CG did not show a significant statistical difference between the results before and after the hematocrit standardization, but these parameters showed a significant improvement in the RBCs deformability after the hematocrit standardization. The same significant differences were not observed in CG, since the change of Hct in CG was only 7% significantly less than the Hct change in FG (approximately 19%).

The weights of the body and organs and the histological examinations

AVF models showed a steady increase in heart and lung weight in proportion to the fistula diameter. [65,109,114,142,143] Many evidences of severe congestive heart failure in the studies are based on the organs weight, e.g. the ratio of heart weight to body weight more than 5 mg /

g or lung weight more than 2.5 g.[109,110] Lung weight increase occurs due to fluid accumulation in the lung or what is called lung congestion especially in the presence of a high flow AVF,[109] but small AVFs did not show the same significant difference in lung weight.[109,114]

The heart weight to body weight ratio in our study was 4.45±0.39 mg/g, mean lung weight was 1.4 g, and no significant difference was observed in lung weight to body weight ratio between FG and SG.

Studies have shown varying results on the effect of arteriovenous fistulas on the body weight. This effect actually differs according to the size of the arteriovenous fistula and the follow-up period after surgery. However, rapid body weight gain after fistula surgery is evidence of fluid retention, and some studies have considered an increase of 50 grams or more within 7 days as evidence of severe heart failure.[143]

Our results showed a slight decrease in the body weight of the rat in the fistula group one week after the creation of the fistula, this loss of weight may be due to the post-operative stress, and the rats regained the weight after 6 weeks without a pathologic significant changes (the weight gain was only 22.7 ± 12.8 g during 6 weeks). The results of our study are consistent with the results of other studies in terms of a temporary decrease after a week of surgery, then a normal weight gain without a statistically significant difference compared to the control group after a month of surgery.[110,114]

The arteriovenous fistula in this model resulted in statistically significant left ventricular hypertrophy compared to the control group due to overloading via the arteriovenous fistula. All these data and the high survival rate refer to significant cardiac pathology induced by CJF but without reaching a severe congestive heart failure at the end-point measurement.

As an additional finding, the histological examination showed an expected intimal hyperplasia in venous limb of fistula in FG compared to the non-operated vein in FG and vein

in SG. We would also recommend this model for studies on intimal hyperplasia in the venous limb of the fistula and its management.

Main findings

- The Carotid-jugular fistula resulted in a significant increase of RBC mass and a significant impairment of RBC deformability. These changes could be one of the pathways through which the fistula influences the microcirculation, which opens the door for further studies on a novel proposal to prevent or reduce fistula-related ischemia by using medications that improve the properties of erythrocytes.
- Carotid-jugular fistula in rats is a feasible model of arteriovenous fistula, especially for studies about fistula-related microcirculatory and systemic changes.
- Carotid-jugular fistula has significant effects on the remote organs, since it results in significant hemodynamic differences, left ventricular hypertrophy and significant alteration of the liver microcirculation.

  The ligation or banding of AVF lead to immediate hemodynamic changes, therefore it should be considered especially in the critical cases.

6. Summary

Arterio-venous fistula (AVF) is the first option for hemodialysis. This study evaluated the carotid-jugular-fistula (CJF) as a model to study fistula-related microcirculatory and systemic changes and presented the hemorheological changes as a suggested mechanism of the impaired tissue perfusion.

Sixteen female Wistar rats were used in this study, ten in fistula-group (FG) and six in sham-operated-group (SG). Carotid-Jugular-Anastomosis was done in FG, while the same vessels were just isolated in SG. The rats were followed-up for 6 weeks. Hematological and hemorheological parameters were measured before the operation, and on 1st and 6th postoperative weeks. Besides hemodynamic parameters, the liver and kidney microcirculation were evaluated using laser Doppler device at the 6th week measurements, and the effects of fistula occlusion on the microcirculation were evaluated as well.

The animals in FG group showed significant decrease in hemodynamic parameters after the fistula. Liver microcirculatory blood flux units (BFU) were significantly lower in FG in comparison with SG and increased significantly after the occlusion of the fistula. Kidney BFU showed closer changes but without significant differences. Erythrocyte deformability significantly impaired in FG after the fistula. Morphologically marked increase in absolute and relative heart weight values was found with left ventricular hypertrophy.

The carotid-jugular fistula acted as a feasible model of AVF. Besides the well-known hemodynamic effects, the presence of the CJF resulted in impaired Erythrocyte deformability and mechanical stability. These changes could be one of the pathways through which the arteriovenous fistula may influence the microcirculation.

7. Bibliography

7.1. References

1. Agarwal AK. Systemic Effects Of Hemodialysis Access. Advances In Chronic Kidney Disease. 2015;22:459–465

2. Basile C, Vernaglione L, Casucci F, Libutti P, Lisi P, Rossi L, Vigo V, et al. The Impact Of Haemodialysis Arteriovenous Fistula On Haemodynamic Parameters Of The Cardiovascular System. Clinical Kidney Journal. 2016;9:729–34

3. Zhou W. Acquired Arteriovenous Fistulae. In: JL C, Johnston KW, eds. Rutherford's Vascular Surgery. Eighth edi. Philadelphia: Elsevier Saunders; 2014:1268–1282

4. Bylsma LC, Gage SM, Reichert H, Dahl SLM, Lawson JH. Arteriovenous Fistulae For Haemodialysis: A Systematic Review And Meta-Analysis Of Efficacy And Safety Outcomes. European Journal Of Vascular And Endovascular Surgery. 2017;54:513–522 doi:10.1016/j.ejvs.2017.06.024

5. Al-Jaishi AA, Liu AR, Lok CE, Zhang JC, Moist LM. Complications Of The Arteriovenous Fistula: A Systematic Review. Journal Of The American Society Of Nephrology. 2017;28:1839–1850 doi:10.1681/ASN.2016040412

6. Huber TS. Hemodialysis Access: General Considerations. In: Cronenwett JL JK, ed. Rutherford's Vascular Surgery. Eighth Edi. Philadelphia: Elsevier Saunders; 2014:1082–1098

7. Yang R, Humphrey S. Review Of Arteriovenous Fistula Care. EDTNA-ERCA Journal. 2000;26:11–14 doi:10.1111/j.1755-6686.2000.tb00069.x

8. Bos WJW, Zietse R, Wesseling KH, Westerhof N. Effects Of Arteriovenous Fistulas On Cardiac Oxygen Supply And Demand. Kidney International. 1999;55:2049–2053

9. Croatt AJ, Grande JP, Hernandez MC, Ackerman AW, Katusic ZS, Nath KA. Characterization Of A Model Of An Arteriovenous Fistula In The Rat: The Effect Of L-NAME. The American Journal Of Pathology. 2010;176:2530–2541

10. Nath KA, Katusic ZS. Predicting The Functionality And Form Of A Dialysis Fistula. Journal Of The American Society Of Nephrology : JASN. 2016;27:3508–3510

11. Lemson M, Zwiers I, Kurvers H, Daemen M, Beuk R, Tordoir J. Prosthetic Arteriovenous Fistulas For Hemodialysis Impair The Macro- And Microcirculation Of The Hand More Than Brescia/Cimino AV Fistulas. Journal Of Vascular Technology. 1997;Volume 21:187–191

12. Harris L. Hemodialysis Access : Nonthrombotic Complications. In: Cronenwett J, Johnston K, eds. Rutherford's Vascular Surgery. Eighth Edi. Philadelphia: Elsevier Saunders; 2014:1135–1152

13. Zanow J, Kruger U, Scholz H. Proximalization Of The Arterial Inflow: A New Technique To Treat Access-Related Ischemia. Journal Of Vascular Surgery. 2006;43:1216–1221

14. Jennings W, Brown R, Blebea J, Taubman K, Messiner R. Prevention Of Vascular Access Hand Ischemia Using The Axillary Artery As Inflow. Journal Of Vascular Surgery. 2013;58:1305–1309

15. Chai C, Sulaiman W, Saad M, Rasool H, Shokri A. Skin Microcirculatory Changes In Relation To Arteriovenous Fistula Maturation. Indian Journal Of Nephrology. 2018;28:421–426

16. Prommer H-U, Maurer J, von Websky K, Freise C, Sommer K, Nasser H, Samapati R, et al. Chronic Kidney Disease Induces A Systemic Microangiopathy, Tissue Hypoxia And Dysfunctional Angiogenesis. Scientific Reports. 2018;8:5317

17. Guven G, Hilty MP, Ince C. Microcirculation: Physiology, Pathophysiology, And Clinical Application. Blood Purification. 2020;49:143–150

18. Malpighius M, Epistel I. About The Lungs. In: Willius F, Keys T, eds. Classics in Cardiology. New York: Henry Schumann Dover Public; 1941:89–97

19. Inoki R, Kudo T, Olgart LM, Okabe E, Todoki K, Ito H. Microcirculation: Function And Regulation In Microvasculature. In: Dynamic Aspects of Dental Pulp. Springer Netherlands; 1990:151–166 doi:10.1007/978-94-009-0421-7_9

20. Bateman M, Sharpe D, Ellis G. Bench-To-Bedside Review: Microvascular Dysfunction In Sepsis - Hemodynamics, Oxygen Transport, And Nitric Oxide. Critical Care. 2003;7:359–373 doi:10.1186/cc2353

21. Den Uil A, Lagrand K, Van Der Ent M, Jewbali D, Cheng M, Spronk E, Simoons L. Impaired Microcirculation Predicts Poor Outcome Of Patients With Acute Myocardial Infarction Complicated By Cardiogenic Shock. European Heart Journal. 2010;31:3032–3039

22. Brahmbhatt A, Remuzzi A, Franzoni M, Misra S. The Molecular Mechanisms Of Hemodialysis Vascular Access Failure. Kidney International. 2016;89:303–316

23. Kameneva M V., Antaki JF. Mechanical Trauma To Blood. In: Baskurt OK, Hardeman MR, Rampling MW, Meiselman HJ, eds. Handbook of Hemorheology and Hemodynamics. Amsterdam: IOS Press; 2007:206–227

24. Baskurt OK. Mechanisms Of Blood Rheology Alterations. In: Baskurt OK, Hardeman MR, Rampling MW, Meiselman HJ, eds. Handbook of Hemorheology and Hemodynamics. Amsterdam: IOS Press; 2007:170–190

25. Bojakowski K, Dzabic M, Kurzejamska E, Styczynski G, Andziak P, Gaciong Z, Söderberg-Nauclér C, et al. A High Red Blood Cell Distribution Width Predicts Failure Of Arteriovenous Fistula. Moura IC, ed. PLoS ONE. 2012;7:e36482

26. Barshtein G, Ben-Ami R, Yedgar S. Role Of Red Blood Cell Flow Behavior In Hemodynamics And Hemostasis. Expert Review Of Cardiovascular Therapy. 2007;5:743–752

27. Sadaghianloo N, Yamamoto K, Bai H, Tsuneki M, Protack CD, Hall MR, Declemy S, et al. Increased Oxidative Stress And Hypoxia Inducible Factor-1 Expression During Arteriovenous Fistula Maturation. Annals Of Vascular Surgery. 2017;41:225–234

28. Misra S, Shergill U, Yang B, Janardhanan R, Misra KD. Increased Expression Of HIF-1alpha, VEGF-A And Its Receptors, MMP-2, TIMP-1, And ADAMTS-1 At The Venous Stenosis Of Arteriovenous Fistula In A Mouse Model With Renal Insufficiency. Journal Of Vascular And Interventional Radiology : JVIR. 2010;21:1255–61

29. Klarik Z, Kiss F, Miko I, Nemeth N. Aorto-Porto-Caval Micro-Rheological Differences

Of Red Blood Cells In Laboratory Rats: Further Deformability And Ektacytometrial Osmoscan Data. Clinical Hemorheology And Microcirculation. 2013;53:217–229

30. Rampling M. Compositional Properties Of Blood. In: Baskurt O, Hardeman M, Rampling M, Meiselman H, eds. Handbook of Hemorheology and Hemodynamics. Amsterdam: IOS Press; 2007:34–44

31. Connes P, Dufour S, Pichon A, Favret F. Blood Rheology, Blood Flow And Human Health. In: Nutrition and Enhanced Sports Performance. Elsevier; 2013:283–293 doi:10.1016/B978-0-12-396454-0.00028-X

32. Schmid-Schönbein H. Microrheology Of Erythrocytes, Blood Viscosity, And The Distribution Of Blood Flow In The Microcirculation. International Review Of Physiology. 1976;9:1–62

33. Jung F, Mrowietz C, Hiebl B, Franke RP, Pindur G, Sternitzky R. Influence Of Rheological Parameters On The Velocity Of Erythrocytes Passing Nailfold Capillaries In Humans. Clinical Hemorheology And Microcirculation. 2011;48:129–39

34. Lipowsky H. Microvascular Rheology And Hemodynamics. Microcirculation. 2005;12:5–15

35. Cho Y-I, Cho DJ. Hemorheology And Microvascular Disorders. Korean Circulation Journal. 2011;41:287–95

36. Baskurt OK, Meiselman HJ. Blood Rheology And Hemodynamics. Seminars In Thrombosis And Hemostasis. 2003;29:435–450

37. Bogár L. Diagnosztika. In: Sándor IB, Pongrácz E, eds. A Klinikai Haemorheologia Alapjai. Budapest: Kornétás Kiadó; 1999:33–50

38. Toth K, Kesmarky G, Alexy T. Clinical Significance Of Hemorheological Alterations. In: Baskurt, Oguz K Hardeman, Max R Rampling, Michael W Meiselman HJ, ed. Handbook of Hemorheology and Hemodynamics. IOS Press. Amsterdam: IOS Press; 2007:392–432

39. HH L. Blood Rheology Aspects Of The Microcirculation. In: Baskurt OK, Hardeman MR, Rampling MW, Meiselman HJ, eds. Handbook of Hemorheology and Hemodynamics. Amsterdam: IOS Press; 2007:307–321

40. Yagi H, Sumino H, Aoki T, Tsunekawa K, Araki O, Kimura T, Nara M, et al. Impaired Blood Rheology Is Associated With Endothelial Dysfunction In Patients With Coronary Risk Factors. Clinical Hemorheology And Microcirculation. 2016;62:139–50

41. Konner K, Nonnast-Daniel B, Ritz E. The Arteriovenous Fistula. Journal Of The American Society Of Nephrology : JASN. 2003;14:1669–80

42. Kremyanskaya M, Najfeld V, Mascarenhas J, Hoffman R. The Polycythemias. In: Hoffman R, ed. Hematology: Basic Principles and Practice. Sixth edit. Philadelphia: Elsevier Saunders; 2009:998–1033

43. Cockelt GR, Meiselman HJ. Macro- And Micro-Rheological Properties Of Blood. In: Baskurt OK, Hardeman MR, Rampling MW, Meiselman HJ, eds. Handbook of Hemorheology and Hemodynamics. Amsterdam: IOS Press; 2007:45–71

44. Mozos I. Mechanisms Linking Red Blood Cell Disorders And Cardiovascular Diseases.

BioMed Research International. 2015

45. Mistrík E, Dusilová Sulková S, Bláha V, Kalousová M, Knízek J, Moucka P, Herout V, et al. Evaluation Of Skin Microcirculation During Hemodialysis. Renal Failure. 2010;32:21–26

46. Yeh C, Chao A, Lee Y, Lee T, Yeh C, Liu M, Tsai K. An Observational Study Of Microcirculation In Dialysis Patients And Kidney Transplant Recipients. European Journal Of Clinical Investigation. 2017;47:630–637

47. Hardeman MR, Goedhart PT, Shin S. Methods In Hemorheology. In: Baskurt OK, Hardeman MR, Rampling MW, Meiselman HJ, eds. Handbook of Hemorheology and Hemodynamics. Amsterdam: IOS Press; 2007:242–266

48. Välisuo P. Optical Methods For Assessing Skin Flap Survival. In: Biophotonics for Medical Applications. Elsevier Inc.; 2015:331–346 doi:10.1016/B978-0-85709-662-3.00012-9

49. Obeid AN, Barnett NJ, Dougherty G, Ward G. A Critical Review Of Laser Doppler Flowmetry. Journal Of Medical Engineering & Technology. 1990;14:178–181

50. Matthews B, Vongsavan N. Advantages And Limitations Of Laser Doppler Flow Meters. International Endodontic Journal. 1993;26:9–9

51. Babos L, Járai Z, Nemcsik J. Evaluation Of Microvascular Reactivity With Laser Doppler Flowmetry In Chronic Kidney Disease. World Journal Of Nephrology. 2013;2:77

52. Hever T, Nemeth N, Brath E, Toth L, Kiss F, Sajtos E, Matyas L, et al. Morphological, Hemodynamical And Hemorheological Changes Of Mature Artificial Saphenous Arterio-Venous Shunts In The Rat Model. Microsurgery. 2010;30:649–656

53. Wattanasirichaigoon S, Pomposelli FB. Branham's Sign Is An Exaggerated Bezold-Jarisch Reflex Of Arteriovenous Fistula. Journal Of Vascular Surgery. 1997;26:171–172

54. Velez-Roa S, Neubauer J, Wissing M, Porta A, Somers VK, Unger P, van de Borne P. Acute Arterio-Venous Fistula Occlusion Decreases Sympathetic Activity And Improves Baroreflex Control In Kidney Transplanted Patients. Nephrology Dialysis Transplantation. 2004;19:1606–1612

55. Kang L, Yamada S, Hernandez MC, Croatt AJ, Grande JP, Juncos JP, Vercellotti GM, et al. Regional And Systemic Hemodynamic Responses Following The Creation Of A Murine Arteriovenous Fistula. American Journal Of Physiology-Renal Physiology. 2011;301:845–851

56. Gomes AC, Falcão-Pires I, Pires AL, Brás-Silva C, Leite-Moreira AF. Rodent Models Of Heart Failure: An Updated Review. Heart Failure Reviews. 2013;18:219–249

57. Zheng C, Zhou Y, Huang C, Zhang Z, Liu YI, Xu Y. Establishment Of A Rat Autogenous Arteriovenous Fistula Model Following 5/6 Nephrectomy. Experimental And Therapeutic Medicine. 2015;10:219–224

58. Rotmans JI. Animal Models For Studying Pathophysiology Of Hemodialysis Access. The Open Urology & Nephrology Journal. 2014;7:14–21

59. Misra S, Fu AA, Anderson JL, Sethi S, Glockner JF, McKusick MA, Bjarnason H, et al. The Rat Femoral Arteriovenous Fistula Model: Increased Expression Of Matrix Metalloproteinase-2 And -9 At The Venous Stenosis. Journal Of Vascular And Interventional Radiology. 2008;19:587–594

60. Beatty JS, Wach PF, Paulson WD, Merchen TD, Pollock DM, Pollock JS, White JJ. Complications Impair The Usefulness And Validity Of The Rat Tail Arteriovenous Fistula Model. Kidney International. 2009;76:916

61. Bojakowski K, Janusz G, Grabowska I, Zegrocka-Stendel O, Surowiecka-Pastewka A, Kowalewska M, Maciejko D, et al. Rat Model Of Parkes Weber Syndrome. PLoS ONE. 2015;10:e0133752

62. Nasir S, Aydin M, Karahan N, Demiryürek D, Sargon M. New Microvenous Anastomosis Model For Microsurgical Training: External Jugular Vein. Journal Of Reconstructive Microsurgery. 2006;22:625–630

63. Payan HM, Conrad JR. Carotid Ligation In Gerbils. Influence Of Age, Sex, And Gonads. Stroke. 1977;8:194–196

64. Morgan MK, Anderson RE, Sundt TM. A Model Of The Pathophysiology Of Cerebral Arteriovenous Malformations By A Carotid-Jugular Fistula In The Rat. Brain Research. 1989;496:241–250

65. Sageshima M, Kawamura K, Toda K, Masuda H, Shozawa T. An Ultrastructural Study Of Pulmonary Capillary Vessels In Blood Volume-Overloaded Rat. Advances In Experimental Medicine And Biology. 1990;277:673–680

66. Sekhon LH, Morgan MK, Spence I, Weber NC. Chronic Cerebral Hypoperfusion: Pathological And Behavioral Consequences. Neurosurgery. 1997;40:548–556

67. Sahara Y, Miyachi S, Nagasaka T, Negoro M, Suzuki O, Hattori K, Kobayashi N, et al. Radiological And Pathological Changes In The Sinus Of An Experimental Arteriovenous Fistula Of The Rat. Interventional Neuroradiology : Journal Of Peritherapeutic Neuroradiology, Surgical Procedures And Related Neurosciences. 2003;9:101–105

68. Tohda K, Masuda H, Kawamura K, Shozawa T. Difference In Dilatation Between Endothelium-Preserved And -Desquamated Segments In The Flow-Loaded Rat Common Carotid Artery. Arteriosclerosis And Thrombosis : A Journal Of Vascular Biology. 1992;12:519–528

69. Lawton MT, Arnold CM, Kim YJ, Bogarin EA, Stewart CL, Wulfstat AA, Derugin N, et al. Radiation Arteriopathy In The Transgenic Arteriovenous Fistula Model. Neurosurgery. 2008;62:1129–38; discussion 138-9

70. Lawton MT, Stewart CL, Wulfstat AA, Derugin N, Hashimoto T, Young WL. The Transgenic Arteriovenous Fistula In The Rat: An Experimental Model Of Gene Therapy For Brain Arteriovenous Malformations. Neurosurgery. 2004;54:1463–71; discussion 1471

71. Shin Y, Nakase H, Nakamura M, Shimada K, Konishi N, Sakaki T. Expression Of Angiogenic Growth Factor In The Rat DAVF Model. Neurological Research. 2007;29:727–33

72. Shin Y, Uranishi R, Nakase H, Sakaki T. [Vascular Endothelial Growth Factor

Expression In The Rat Dural Arteriovenous Fistula Model]. No To Shinkei = Brain And Nerve. 2003;55:946–52

73. Zhu Y, Lawton MT, Du R, Shwe Y, Chen Y, Shen F, Young WL, et al. Expression Of Hypoxia-Inducible Factor-1 And Vascular Endothelial Growth Factor In Response To Venous Hypertension. Neurosurgery. 2006;59:687–96; discussion 687-96

74. Yamada M, Yuzawa I, Fujii K. Iodoamphetamine (IMP) Uptake In The Brain Is Increased After Experimental Cerebral Venous Hypertension In The Rat. Acta Neurochirurgica Supplement. 2003;86:209–12

75. Herman JM, Spetzler RF, Bederson JB, Kurbat JM, Zabramski JM. Genesis Of A Dural Arteriovenous Malformation In A Rat Model. Journal Of Neurosurgery. 1995;83:539–45

76. Bederson JB, Wiestler OD, Brüstle O, Roth P, Frick R, Yaşargil MG. Intracranial Venous Hypertension And The Effects Of Venous Outflow Obstruction In A Rat Model Of Arteriovenous Fistula. Neurosurgery. 1991;29:341–50

77. Irikura K, Morii S, Miyasaka Y, Yamada M, Tokiwa K, Yada K. Impaired Autoregulation In An Experimental Model Of Chronic Cerebral Hypoperfusion In Rats. Stroke. 1996;27:1399–404

78. Morgan MK, Sundt TM, Anderson RE, Weber N. The Haemodynamic Consequences Of A Carotid-Jugular Fistula In The Rat During Hypocapnia. Journal Of Clinical Neuroscience : Official Journal Of The Neurosurgical Society Of Australasia. 1994;1:193–6

79. Morgan MK, Anderson RE, Sundt TM. The Effects Of Hyperventilation On Cerebral Blood Flow In The Rat With An Open And Closed Carotid-Jugular Fistula. Neurosurgery. 1989;25:606–11; discussion 611-2

80. Morgan MK, Johnston I, Besser M, Baines D. Cerebral Arteriovenous Malformations, Steal, And The Hypertensive Breakthrough Threshold. An Experimental Study In Rats. Journal Of Neurosurgery. 1987;66:563–7

81. Raoufi Rad N, McRobb LS, Zhao Z, Lee VS, Patel NJ, Qureshi AS, Grace M, et al. Phosphatidylserine Translocation After Radiosurgery In An Animal Model Of Arteriovenous Malformation. Radiation Research. 2017;187:701–707

82. Yassari R, Sayama T, Jahromi BS, Aihara Y, Stoodley M, Macdonald RL. Angiographic, Hemodynamic And Histological Characterization Of An Arteriovenous Fistula In Rats. Acta Neurochirurgica. 2004;146:495–504

83. Kashba SR, Patel NJ, Grace M, Lee VS, Raoufi-Rad N, Amal Raj J V., Duong TTH, et al. Angiographic, Hemodynamic, And Histological Changes In An Animal Model Of Brain Arteriovenous Malformations Treated With Gamma Knife Radiosurgery. Journal Of Neurosurgery. 2015;123:954–960

84. Terada T, Higashida RT, Halbach V V, Dowd CF, Tsuura M, Komai N, Wilson CB, et al. Development Of Acquired Arteriovenous Fistulas In Rats Due To Venous Hypertension. Journal Of Neurosurgery. 1994;80:884–9

85. Ng K, Higurashi M, Uemiya N, Qian Y. Secondary Histomorphological Changes In Cerebral Arteries Of Normotensive And Hypertensive Rats Following A Carotid-Jugular Fistula Induction. PloS One. 2014;9:e92433

86. Tu J, Karunanayaka A, Windsor A, Stoodley MA. Comparison Of An Animal Model Of Arteriovenous Malformation With Human Arteriovenous Malformation. Journal Of Clinical Neuroscience. 2010;17:96–102

87. Tu J, Li Y, Hu Z, Chen Z. Radiosurgery Inhibition Of The Notch Signaling Pathway In A Rat Model Of Arteriovenous Malformations. Journal Of Neurosurgery. 2014;120:1385–96

88. Karunanyaka A, Tu J, Watling A, Storer KP, Windsor A, Stoodley MA. Endothelial Molecular Changes In A Rodent Model Of Arteriovenous Malformation. Journal Of Neurosurgery. 2008;109:1165–1172

89. Storer K, Tu J, Karunanayaka A, Smee R, Short R, Thorpe P, Stoodley M. Coadministration Of Low-Dose Lipopolysaccharide And Soluble Tissue Factor Induces Thrombosis After Radiosurgery In An Animal Arteriovenous Malformation Model. Neurosurgery. 2007;61:604–10; discussion 610-1

90. Hai J, Wan J-F, Lin Q, Wang F, Zhang L, Li H, Zhang L, et al. Cognitive Dysfunction Induced By Chronic Cerebral Hypoperfusion In A Rat Model Associated With Arteriovenous Malformations. Brain Research. 2009;1301:80–8

91. Hai J, Lin Q, Deng D-F, Pan Q-G, Ding M-X. The Pre-Treatment Effect On Brain Injury During Restoration Of Normal Perfusion Pressure With Hemodilution In A New Rat Model Of Chronic Cerebral Hypoperfusion. Neurological Research. 2007;29:583–7

92. Hai J, Li S-T, Lin Q, Pan Q-G, Gao F, Ding M-X. Vascular Endothelial Growth Factor Expression And Angiogenesis Induced By Chronic Cerebral Hypoperfusion In Rat Brain. Neurosurgery. 2003;53:963–70; discussion 970-2

93. Hai J, Ding M, Guo Z, Wang B. A New Rat Model Of Chronic Cerebral Hypoperfusion Associated With Arteriovenous Malformations. Journal Of Neurosurgery. 2002;97:1198–202

94. Yang S-T, Rodriguez-Hernandez A, Walker EJ, Young WL, Su H, Lawton MT. Adult Mouse Venous Hypertension Model: Common Carotid Artery To External Jugular Vein Anastomosis. Journal Of Visualized Experiments. 2015:50472

95. Kojima T, Miyachi S, Sahara Y, Nakai K, Okamoto T, Hattori K, Kobayashi N, et al. The Relationship Between Venous Hypertension And Expression Of Vascular Endothelial Growth Factor: Hemodynamic And Immunohistochemical Examinations In A Rat Venous Hypertension Model. Surgical Neurology. 2007;68:277–84; discussion 284

96. Geenen IL, Kolk FF, Molin DG, Wagenaar A, Compeer MG, Tordoir JH, Schurink GW, et al. Nitric Oxide Resistance Reduces Arteriovenous Fistula Maturation In Chronic Kidney Disease In Rats. Jourd'heuil D, ed. PloS One. 2016;11:e0146212

97. Chien C-T, Fan S-C, Lin S-C, Kuo C-C, Yang C-H, Yu T-Y, Lee S-P, et al. Glucagon-Like Peptide-1 Receptor Agonist Activation Ameliorates Venous Thrombosis-Induced Arteriovenous Fistula Failure In Chronic Kidney Disease. Thrombosis And Haemostasis. 2014;112:1051–1064

98. Chou T-F, Chen Y-S, Yu C-C, Chien C-T, Chen C-F. Simple Methods To Elevate Pulmonary Arterial Pressure By Pre- And Post-Tricuspid Shunts In Rats. The Chinese Journal Of Physiology. 2002;45:131–135

99. Skillicorn CJ. Do The Terms “Proximal” And “Distal” Cause Confusion Amongst Radiologists And Other Clinicians? Clinical Radiology. 2009;64:397–402

100. Wang X, Ren B, Liu S, Sentex E, Tappia PS, Dhalla NS. Characterization Of Cardiac Hypertrophy And Heart Failure Due To Volume Overload In The Rat. Journal Of Applied Physiology. 2003;94:752–763

101. Bachour SP, Hevesi M, Bachour O, Sweis BM, Mahmoudi J, Brekke JA, Divani AA. Comparisons Between Garcia, Modo, And Longa Rodent Stroke Scales: Optimizing Resource Allocation In Rat Models Of Focal Middle Cerebral Artery Occlusion. Journal Of The Neurological Sciences. 2016;364:136–140

102. Garcia JH, Wagner S, Liu KF, Hu XJ. Neurological Deficit And Extent Of Neuronal Necrosis Attributable To Middle Cerebral Artery Occlusion In Rats. Statistical Validation. Stroke. 1995;26:627–634

103. Ruan J, Yao Y. Behavioral Tests In Rodent Models Of Stroke. Brain Hemorrhages. 2020

104. Desland FA, Afzal A, Warraich Z, Mocco J. Manual Versus Automated Rodent Behavioral Assessment: Comparing Efficacy And Ease Of Bederson And Garcia Neurological Deficit Scores To An Open Field Video-Tracking System. Journal Of Central Nervous System Disease. 2014;6:JCNSD.S13194

105. Finkelstein A. Design And Evaluation Of A New Diagnostic Instrument For Osmotic Gradient Ektacytometrie. Electronics, Université Paris-Es. 2017

106. Baskurt OK, Hardeman MR, Uyuklu M, Ulker P, Cengiz M, Nemeth N, Shin S, et al. Parameterization Of Red Blood Cell Elongation Index – Shear Stress Curves Obtained By Ektacytometry. Scandinavian Journal Of Clinical And Laboratory Investigation. 2009;69:777–788

107. Baskurt OK, Meiselman HJ. Data Reduction Methods For Ektacytometry In Clinical Hemorheology. Clinical Hemorheology And Microcirculation. 2013;54:99–107

108. Baskurt OK, Meiselman HJ. Red Blood Cell Mechanical Stability Test. Clinical Hemorheology And Microcirculation. 2013;55:55–62

109. Langenickel T, Pagel I, Höhnel K, Dietz R, Willenbrock R. Differential Regulation Of Cardiac ANP And BNP MRNA In Different Stages Of Experimental Heart Failure. American Journal Of Physiology Heart And Circulatory Physiology. 2000;278:1500–1506

110. Treskatsch S, Feldheiser A, Rosin AT, Sifringer M, Habazettl H, Mousa SA, Shakibaei M, et al. A Modified Approach To Induce Predictable Congestive Heart Failure By Volume Overload In Rats. PLoS ONE. 2014;9:1–7

111. Jennings WC, Taubman KE. Alternative Autogenous Arteriovenous Hemodialysis Access Options. Seminars In Vascular Surgery. 2011;24:72–81

112. Yamamoto K, Li X, Shu C, Miyata T, Dardik A. Technical Aspects Of The Mouse Aortocaval Fistula. Journal Of Visualized Experiments : JoVE. 2013:50449

113. Mickle JP, Menges JT, Day AL, Quisling R, Ballinger W. Experimental Aortocaval Fistulae In Rats. Microsurgery. 1981;2:283–288

114. Liu Z, Hilbelink DR, Crockett WB, Gerdes AM. Regional Changes In Hemodynamics

And Cardiac Myocyte Size In Rats With Aortocaval Fistulas. 1. Developing And Established Hypertrophy. Circulation Research. 1991;69:52–58

115. Ozek C, Zhang F, Lineaweaver WC, Chin BT, Eiman T, Newlin L, Buncke HJ. A New Heart Failure Model In Rat By An End-To-Side Femoral Vessel Anastomosis. Cardiovascular Research. 1998;37:236–238

116. Langer S, Heiss C, Paulus N, Bektas N, Mommertz G, Rowinska Z, Westenfeld R, et al. Functional And Structural Response Of Arterialized Femoral Veins In A Rodent AV Fistula Model. Nephrology Dialysis Transplantation. 2009;24:2201–2206

117. Aalbers MW, Rijkers K, van Winden LAAP, Hoogland G, Vles JSH, Majoie HJM. Horner's Syndrome: A Complication Of Experimental Carotid Artery Surgery In Rats. Autonomic Neuroscience. 2009;147:64–69

118. Iwashima Y, Horio T, Takami Y, Inenaga T, Nishikimi T, Takishita S, Kawano Y. Effects Of The Creation Of Arteriovenous Fistula For Hemodialysis On Cardiac Function And Natriuretic Peptide Levels In CRF. American Journal Of Kidney Diseases. 2002;40:974–982

119. Huang M, Hester RL, Guyton AC. Hemodynamic Changes In Rats After Opening An Arteriovenous Fistula. The American Journal Of Physiology. 1992;262:846–851

120. Flaim SF, Minteer WJ, Nellis SH, Clark DP. Chronic Arteriovenous Shunt: Evaluation Of A Model For Heart Failure In Rat. American Journal Of Physiology-Heart And Circulatory Physiology. 1979;236:H698–H704

121. Azar T, Sharp J, Lawson D. Heart Rates Of Male And Female Sprague-Dawley And Spontaneously Hypertensive Rats Housed Singly Or In Groups. Journal Of The American Association For Laboratory Animal Science. 2011;50:175–184

122. Velez-Roa S, Neubauer J, Wissing M, Porta A, Somers VK, Unger P, van de Borne P. Acute Arterio-Venous Fistula Occlusion Decreases Sympathetic Activity And Improves Baroreflex Control In Kidney Transplanted Patients. Nephrology Dialysis Transplantation. 2004;19:1606–1612

123. Haase VH. Hypoxic Regulation Of Erythropoiesis And Iron Metabolism. American Journal Of Physiology Renal Physiology. 2010;299:F1-13

124. Haase VH. Regulation Of Erythropoiesis By Hypoxia-Inducible Factors. Blood Reviews. 2013;27:41–53

125. Stolic R. Most Important Chronic Complications Of Arteriovenous Fistulas For Hemodialysis. Medical Principles And Practice. 2013;22:220–228

126. Misra S, Fu AA, Rajan DK, Juncos LA, McKusick MA, Bjarnason H, Mukhopadhyay D. Expression Of Hypoxia Inducible Factor–1α, Macrophage Migration Inhibition Factor, Matrix Metalloproteinase–2 And −9, And Their Inhibitors In Hemodialysis Grafts And Arteriovenous Fistulas. Journal Of Vascular And Interventional Radiology. 2008;19:252–259

127. Stumpe KO, Sölle H, Klein H, Krück F. Mechanism Of Sodium And Water Retention In Rats With Experimental Heart Failure. Kidney International. 1973;4:309–17

128. Rosenberger C, Mandriota S, Jürgensen JS, Wiesener MS, Hörstrup JH, Frei U, Ratcliffe PJ, et al. Expression Of Hypoxia-Inducible Factor-1alpha And -2alpha In Hypoxic And

Ischemic Rat Kidneys. Journal Of The American Society Of Nephrology : JASN. 2002;13:1721–32

129. Prchal JT. Primary And Secondary Erythrocytoses. In: Kaushansky K, Prchal JT, Press OW, et al., eds. Williams Hematology. Ninth Edit. by McGraw-Hill Education; 2016:871–888

130. Kadikoylu G, Yavasoglu I, Bolaman Z, Senturk T. Platelet Parameters In Women With Iron Deficiency Anemia. Journal Of The National Medical Association. 2006;98:398–402

131. Zandecki M, Genevieve F, Gerard J, Godon A. Spurious Counts And Spurious Results On Haematology Analysers: A Review. Part I: Platelets. Clinical And Laboratory Haematology. 2007;29:4–20

132. Buss DH, Cashell AW, O'Connor ML, Richards F, Case LD. Occurrence, Etiology, And Clinical Significance Of Extreme Thrombocytosis: A Study Of 280 Cases. The American Journal Of Medicine. 1994;96:247–53

133. Nemeth N, Lesznyak T, Szokoly M, Furka I, Miko I. Allopurinol Prevents Erythrocyte Deformability Impairing But Not The Hematological Alterations After Limb Ischemia–Reperfusion In Rats. Journal Of Investigative Surgery. 2006;19:47–56

134. Li N, Zhou H, Tang Q. Red Blood Cell Distribution Width: A Novel Predictive Indicator For Cardiovascular And Cerebrovascular Diseases. Disease Markers. 2017;2017:1–23

135. Memetoğlu ME, Kehlibar T, Yilmaz M, Kocaaslan C, Günay R, Arslan İY, Ketenci B, et al. Red Blood Cell Distribution Width Is Associated With Early Failure Of Arteriovenous Fistula For Haemodialysis Access. Blood Coagulation & Fibrinolysis. 2015;26:32–35

136. Vaya A, Hernández JL, Zorio E, Bautista D. Association Between Red Blood Cell Distribution Width And The Risk Of Future Cardiovascular Events. Clinical Hemorheology And Microcirculation. 2012;50:221–225

137. Felker GM, Allen LA, Pocock SJ, Shaw LK, McMurray JJV, Pfeffer MA, Swedberg K, et al. Red Cell Distribution Width As A Novel Prognostic Marker In Heart Failure. Data From The CHARM Program And The Duke Databank. Journal Of The American College Of Cardiology. 2007;50:40–47

138. Vayá A, Alis R, Suescún M, Rivera L, Murado J, Romagnoli M, Solá E, et al. Association Of Erythrocyte Deformability With Red Blood Cell Distribution Width In Metabolic Diseases And Thalassemia Trait. Clinical Hemorheology And Microcirculation. 2016;61:407–415

139. Vayá A, Rivera L, De La Espriella R, Sanchez F, Suescun M, Hernandez JL, Fácila L. Red Blood Cell Distribution Width And Erythrocyte Deformability In Patients With Acute Myocardial Infarction. Clinical Hemorheology And Microcirculation. 2015;59:107–114

140. Patel K V., Mohanty JG, Kanapuru B, Hesdorffer C, Ershler WB, Rifkind JM. Association Of The Red Cell Distribution Width With Red Blood Cell Deformability. In: Adv Exp Med Biol.Vol 765.; 2013:211–216 doi:10.1007/978-1-4614-4989-8_29

141. Dobbe JGG, Streekstra GJ, Hardeman MR, Ince C, Grimbergen CA. Measurement Of The Distribution Of Red Blood Cell Deformability Using An Automated Rheoscope.

Clinical Cytometry. 2002;50:313–325

142. Huang M, LeBlanc MH, Hester RL. Evaluation Of The Needle Technique For Producing An Arteriovenous Fistula. Journal Of Applied Physiology (Bethesda, Md : 1985). 1994;77:2907–2911

143. Brower GL, Janicki JS. Contribution Of Ventricular Remodeling To Pathogenesis Of Heart Failure In Rats. American Journal Of Physiology - Heart And Circulatory Physiology. 2001;280:674–683

7.2. Authenticated list of Candidate´s Publications

UNIVERSITY of DEBRECEN

UNIVERSITY AND NATIONAL LIBRARY
UNIVERSITY OF DEBRECEN
H-4002 Egyetem tér 1, Debrecen
Phone: +3652/410-443, email: publikaciok@lib.unideb.hu

Registry number: DEENK/39/2021.PL
Subject: PhD Publication List

Candidate: Souleiman Ghanem
Doctoral School: Doctoral School of Clinical Medicine

List of publications related to the dissertation

1. **Ghanem, S.**, Somogyi, V., Tánczos, B., Szabó, B., Deák, Á., Németh, N.: Modulation of micro-rheological and hematological parameters in the presence of artificial carotid-jugular fistula in rats.
   Clin. Hemorheol. Microcirc. 71 (3), 325-335, 2019.
   DOI: http://dx.doi.org/10.3233/CH-180411
   IF: 1.741

2. **Ghanem, S.**, Tánczos, B., Deák, Á., Bidiga, L., Németh, N.: Carotid-Jugular Fistula Model to Study Systemic Effects and Fistula-Related Microcirculatory Changes.
   J. Vasc. Res. 55 (5), 268-277, 2018.
   DOI: http://dx.doi.org/10.1159/000491930
   IF: 1.855

List of other publications

3. Szabó, B., Fazekas, L., **Ghanem, S.**, Godó, Z., Madar, J., Apró, A., Németh, N.: Biomechanical comparison of microvascular anastomoses prepared by various suturing techniques.
   Injury-Int. J. Care Inj. 51 (12), 2866-2873, 2020.
   DOI: http://dx.doi.org/10.1016/j.injury.2020.02.104
   IF: 2.106 (2019)

4. Szabó, B., Tánczos, B., Varga, Á., Baráth, B., **Ghanem, S.**, Rezsabek, Z., Al-Smadi, M., W., Németh, N.: Micro-rheological changes of red blood cells in the presence of an arterio-venous fistula or a loop-shaped venous graft in the rat.
   Front. Physiol. 11, 1-12, 2020.
   DOI: http://dx.doi.org/10.3389/fphys.2020.616528
   IF: 3.367 (2019)

5. **Ghanem, S.**, Lesznyák, T., Fazekas, L., Tánczos, B., Baráth, B., Nasser, M., Horváth, L., Bidiga, L., Szabó, B., Deák, Á., Pető, K., Németh, N.: Microrheology, microcirculation and structural compensatory mechanisms of a chronic kidney disease rat model: a preliminary study.
Clin. Hemorheol. Microcirc. 75 (1), 47-56, 2020.
DOI: http://dx.doi.org/10.3233/CH-190763
IF: 1.741 (2019)

6. Varga, G., **Ghanem, S.**, Szabó, B., Nagy, K., Pál, N., Tánczos, B., Somogyi, V., Baráth, B., Deák, Á., Matolay, O., Bidiga, L., Pető, K., Németh, N.: Which remote ischemic preconditioning protocol is favorable in renal ischemia-reperfusion injury in the rat?
Clin. Hemorheol. Microcirc. 76 (3), 439-451, 2020.
DOI: http://dx.doi.org/10.3233/CH-200916
IF: 1.741 (2019)

7. Nemes, B. Á., Pető, K., Németh, N., Mester, A., Magyar, Z., **Ghanem, S.**, Somogyi, V., Tánczos, B., Deák, Á., Kállay, M., Bidiga, L., Frecska, E.: N,N-dimethyltryptamine Prevents Renal Ischemia-Reperfusion Injury in a Rat Model.
Transplant. Proc. 51 (4), 1268-1275, 2019.
DOI: http://dx.doi.org/10.1016/j.transproceed.2019.04.005
IF: 0.784

8. Varga, G., **Ghanem, S.**, Szabó, B., Nagy, K., Pál, N., Tánczos, B., Somogyi, V., Baráth, B., Deák, Á., Pető, K., Németh, N.: Renal ischemia-reperfusion-induced metabolic and micro-rheological alterations and their modulation by remote organ ischemic preconditioning protocols in the rat.
Clin. Hemorheol. Microcirc. 71 (2), 225-236, 2019.
DOI: http://dx.doi.org/10.3233/CH-189414
IF: 1.741

9. Magyar, Z., Mester, A., Nadubinszky, G., Varga, G., **Ghanem, S.**, Somogyi, V., Tánczos, B., Deák, Á., Bidiga, L., Mihai, O., Pető, K., Németh, N.: Beneficial effects of remote organ ischemic preconditioning on micro-rheological parameters during liver ischemia-reperfusion in the rat.
Clin. Hemorheol. Microcirc. 70 (2), 181-190, 2018.
DOI: http://dx.doi.org/10.3233/CH-170351
IF: 1.642

10. Pető, K., Németh, N., Mester, A., Magyar, Z., **Ghanem, S.**, Somogyi, V., Tánczos, B., Deák, Á., Bidiga, L., Frecska, E., Nemes, B. Á.: Hemorheological and metabolic consequences of renal ischemia-reperfusion and their modulation by N,N-dimethyltryptamine on a rat model.
Clin. Hemorheol. Microcirc. 70 (1), 107-117, 2018.
DOI: http://dx.doi.org/10.3233/CH-170361
IF: 1.642

UNIVERSITY AND NATIONAL LIBRARY
UNIVERSITY OF DEBRECEN
H-4002 Egyetem tér 1, Debrecen
Phone: +3652/410-443, email: publikaciok@lib.unideb.hu

11. Magyar, Z., Varga, G., Mester, A., **Ghanem, S.**, Somogyi, V., Tánczos, B., Deák, Á., Bidiga, L., Pető, K., Németh, N.: Is the early or delayed remote ischemic preconditioning the more effective from a microcirculatory and histological point of view in a rat model of partial liver ischemia-reperfusion?
Acta Cir. Bras. 33 (7), 597-608, 2018.
DOI: http://dx.doi.org/10.1590/s0102-865020180070000005
IF: 0.931

Total IF of journals (all publications): 19,291
Total IF of journals (publications related to the dissertation): 3,596

The Candidate's publication data submitted to the iDEa Tudóstér have been validated by DEENK on the basis of the Journal Citation Report (Impact Factor) database.

28 January, 2021

DEBRECENI EGYETEM
Egyetemi és Nemzeti Könyvtár

8. Keywords

Carotid-jugular fistula

Arteriovenous fistula

Microcirculation

Laser Doppler

Remote organs

Hematology

Hemorheology

Red blood cell deformability

Mechanical stability

9. Acknowledgements

I would like to express my special thanks of gratitude to Hungary and to the Stipendium Hungaricum Scholarship for offering me and many of my colleagues this chance to pursue our study here at the University of Debrecen. It was a golden chance and a turning point in my life.

I also would like to extend my gratitude to all the staff of the Department of Operative Techniques and Surgical Research who hosted me like a family.

My great thanks to Professor Norbert Nemeth who kindly supervised and enriched with his experiences this academic work. It was a big honor for me to work with you. Thanks for your guidance, patience and big support.

My sincere appreciation; to Prof. Irén Mikó and Prof. István Furka for their great efforts for our department and for their helpful advices and comments, and to Dr. Pető Katalin and Dr. Deák Ádám for their kindness and support.

A special thank goes to Gödényné Rozália, you were a guardian angel offering your limitless help to all of us.

Debrecen, my second home, my words cannot depict your beauty. I will long for your quite nights, for your lively festivals, for all the details passed through my life there.

My very precious father, mother, sister, and brothers; thanks for your unconditional love and endless support. You have been always the reason behind my success.

For a warm heart, full of life, beating with love thank you always for being by my side.

10. Appendix

PUBLICATIONS RELATED TO THE DISSERTATION